Pergamon

Geochimica et Cosmochimica Acta, Vol. 65, No. 16, pp. 2691–2708, 2001

0016-7037/01 $20.00 + .00

PII S0016-7037(01)00614-7

Complexation of metal ions in brines: application of electronic spectroscopy in the study of the Cu(II)-LiCl-H_2O system between 25 and 90°C

JOËL BRUGGER,[1,*], D. C. MCPHAIL,[1] JAY BLACK,[1] and LEONE SPICCIA[2]

[1]Department of Earth Sciences, P.O. Box 28E, Monash University, Victoria, Australia 3800
[2]Department of Chemistry, Monash University, Victoria, Australia 3800

(*Received September* 7, 2000; *accepted in revised form February* 12, 2001

Abstract—The concentration and transport of metals in hydrothermal solutions depend on how metals ions combine with ligands to form complexes, and experimental methods are necessary to identify the important complexes. UV-Vis-NIR spectrophotometry was used to study the formation of Cu(II)-chloride complexes in LiCl brines up to very high chlorinities (18 m LiCl), at temperatures between 25°C and 90°C. The number of Cu(II)-chloride complexes necessary to account for the variation in spectra with varying chloride molality at each temperature was estimated using principal component analysis. The molar absorptivity coefficients and concentrations of each complex were then determined using a "model-free" analysis, which does not require any assumption about the chemistry of the system, other than the number of absorbing species present. Subsequently, the results from the "model-free" analysis were integrated with independent experimental evidence to develop a thermodynamic speciation model, where the logarithms of the equilibrium constants for Cu(II)-chloride formation reactions were fitted to the data using a non-linear least-squares approach. Maps of the residual function were used to estimate uncertainties in the fitted equilibrium constants.

The results of this study are similar to published properties of distorted octahedral $[CuCl(OH_2)_5]^+$ and $[CuCl_2(OH_2)_4]^0$ at all temperatures, but diverge for $[CuCl_3(OH_2)_3]^-$ and distorted tetrahedral $[CuCl_4]^{2-}$. Moreover, the data suggest the presence of $[CuCl_5]^{3-}$, probably with D_{3h} point group, at very high salt concentration. This study demonstrates that it is possible to determine apparent thermodynamic equilibrium constants for the formation of complexes of trace amount of metals in highly concentrated brines, such as those associated with many ore deposits. The results are dependent on the choice of activity coefficients for charged and neutral aqueous complexes, but this influence is relatively small compared with the experimental uncertainty. This study shows that Cu^{2+} chloro-complexes, predominantly $[CuCl_2(OH_2)_4]^0$ and $[CuCl_4]^{2-}$, will play a dominant role in nature where free oxygen is available (near-surface), and where chloride activities are very high (evaporitic basins; hypersaline soils).

1. INTRODUCTION

The rapid development of numerical modelling methods and computer technology provides geologists, other scientists and engineers with the capability to produce increasingly accurate simulations of reactive fluid transport. However, these models are dependent on reliable thermodynamic properties for relevant aqueous, vapour and mineral species. Measuring reliable thermodynamic properties for aqueous complexes at relevant temperatures is a difficult and time-consuming task, and few data are available for the geologically important complexes of many metals. Semiempirical predictions from low-temperature data provide one way to estimate the properties of aqueous species at elevated pressures and temperatures (e.g., Anderson et al., 1991; Gu et al., 1994; Sverjensky et al., 1997); however, the further development of these extrapolation methods relies upon the availability of high quality experimental data. For example, recent experimental investigations of Cu(I)-Cl complexes (Xiao et al., 1998) revealed significant discrepancies between the predicted (Sverjensky et al., 1997) and measured dissociation constants for the $[CuCl]_{aq}$ and $[CuCl_2]^-_{aq}$ complexes. Another important gap in our present understanding of metal transport in hydrothermal brines stems from the difficulty in understanding the properties of concentrated electrolyte solutions, and in particular the inability to model the complexation of trace amounts of metal ions in such solutions (e.g., Helgeson and Kirkham, 1974b; Millero et al., 1995). Concentrated brines play a central role in the formation of major types of ore deposits. For example, the brines associated with low temperature (~100–150°C) Mississippi Valley Type deposits typically contain more than 15 wt.% (sometimes as much as 30 wt.%) equivalent NaCl (Roedder, 1976), and those from medium- to high-temperature (250–650°C) porphyry copper deposits can contain more than 60 wt.% equivalent NaCl (e.g., Ulrich et al., 1999).

The present paper is part of on-going work dedicated to understanding the chemistry of Cu(I) and Cu(II) complexes in aqueous and vapour phases in a range of geological environments, e.g., sedimentary, epithermal and magmatic. In this paper we report the results of an UV-Vis-NIR experimental study of Cu(II)-chloride complexes in LiCl brines at the temperatures of 25, 60 and 90°C, and at LiCl concentrations varying between 0 and ~18.5 m (0–44 wt.% LiCl). LiCl was chosen because of its high solubility at room temperature and the availability of density and isopiestic measurements up to 100°C. This allows us to study copper-chloride complexing in solutions with high chloride concentrations typical of some geological environments. Studying metal complexing over wide ranges of ligand concentrations also helps in isolating

*Author to whom correspondence should be addressed (joelb@mail.earth.monash.edu.au).

Table 1. Concentrations of Cu, Cl, and Li in solutions used for measuring UV-Vis-NIR spectra.

	Vis-NIR spectra			UV-Vis spectra		
	Cu [10^{-3} m]	Cl [m]	Li [m]	Cu [10^{-4} m]	Cl [m]	Li [m]
1	8.29	0.101	0.079[a]	4.81	0.0048	—
2	8.29	0.128	0.106[a]	4.82	0.0444	0.0396
3	8.31	0.173	0.151[b]	4.83	0.0881	0.0833
4	8.35	0.327	0.305[b]	4.83	0.0984	0.0936
5	8.37	0.421	0.399[b]	4.84	0.157	0.152
6	8.41	0.545	0.523	4.89	0.300	0.295
7	8.47	0.784	0.762	4.89	0.402	0.397
8	8.54	1.05	1.03	4.90	0.501	0.496
9	8.59	1.24	1.22	4.95	0.750	0.745
10	8.64	1.43	1.41	5.00	1.01	1.00
11	8.75	1.84	1.82	5.03	1.20	1.19
12	8.86	2.26	2.24	5.09	1.50	1.49
13	8.94	2.55	2.52	5.14	1.80	1.80
14	9.02	2.85	2.83	5.18	2.01	2.00
15	9.14	3.31	3.28	5.31	2.56	2.55
16	9.21	3.57	3.55	5.40	3.01	3.00
17	9.34	4.06	4.04	5.49	3.50	3.49
18	9.61	5.09	5.07	5.63	4.20	4.19
19	10.4	8.14	8.12	5.74	4.75	4.74
20	11.1	10.7	10.6	5.77	5.013	5.01
21	12.0	14.2	14.2	5.88	5.51	5.50
22	12.7	16.8	16.7	6.08	6.50	6.49
23	13.2	18.5	18.4	6.37	8.04	8.03
24				6.66	9.50	9.49
25				6.95	11.02	11.0
26				7.33	13.0	13.0
27				7.82	15.5	15.5
28				8.33	18.1	18.1

[a] spectra collected only at 90°C, [b] spectra collected only at 25 and 90°C.

individual aqueous complexes so that their thermodynamic properties can be measured well. The results of our study can be used to predict the behaviour of copper in chloride-bearing waters and brines (e.g., NaCl-dominant) for a wide range of geological and other environments.

The aims of this paper are to:

1. Emphasise the usefulness of UV-Vis spectroscopy in identifying transition-metal aqueous complexes in dilute and concentrated chloride brines;
2. Demonstrate an integrated method of interpreting spectrophotometric data quantitatively to derive reliable thermodynamic properties of aqueous complexes;
3. Provide the data necessary for subsequent UV-Vis studies of Cu(I)-chloride complexes (i.e., so that we can identify and correct spectra for the presence of oxidised Cu(II) complexes); and
4. Measure and discuss the complexing of Cu(II) with chloride and its relevance to the transport of copper in oxidised (e.g., near-surface) geological environments.

2. EXPERIMENTAL METHODS AND DATA PREPARATION

All solutions were prepared from reagent-grade quality chemicals and doubly-deionised water (Millipore Milli-Q®). Two sets of solutions with different copper concentrations were prepared (Table 1) because of the different absorbance of the Cu(II)-complexes in the UV-Vis ($[Cu]_{tot} \approx 5 \cdot 10^{-4}$ m) and Vis-NIR ($[Cu]_{tot} \approx 10^{-2}$ m) regions. In both sets of solutions, two end-member stock solutions were prepared gravimetrically with the same concentration of copper ($CuCl_2 0.2H_2O$; BHD AnalR®), 0 and 18.5 molal LiCl (SigmaUltra® anhydrous, > 99%), respectively, and acidified with concentrated HCl to a pH between 3 and 4 to prevent formation of Cu(II)-hydroxy-complexes. Solutions with intermediate concentrations of LiCl were prepared by mixing (by weight for accuracy) the two end-member stock solutions. UV-Vis-NIR spectra were recorded on a Varian CARY 5G spectrometer using rectangular "suprasyl" quartz cells (path-length 1 cm) and 1 nm increments between 170 nm and 1300 nm. Dual-beam mode was used where the reference cell contained the same electrolyte solution as the sample cell minus the copper. A baseline correction for detector response and anomalies in cell geometry was applied off-line by subtracting a spectrum collected with the same cells, both loaded with solutions that had the same concentrations of LiCl and HCl. The baseline spectra showed no variation between 25 and 90°C, so the baseline spectra measured at 25°C were used at all temperatures.

The recorded absorbance values varied between 0 and 2.5 absorbance units, where the reproducibility was approximately 0.01 absorbance unit. The baseline-corrected spectra were smoothed using a spline (standard deviation 0.01 absorbance unit), and converted from wavelength to wavenumber and from observed absorbance to molar absorbance. In the LiCl-dominated solutions considered here, the molar to molal conversion

Table 2. Power series equation describing the density of a LiCl aqueous solution [$P_{LiCl}(m_{LiCl}, T)$] between 0.1 m and 20 m LiCl, and between 5°C and 100°C.

Coefficient	Factor
0.987033	
0.0237957	m
−0.000606358	m^2
$8.29409\ 10^{-6}$	m^3
0.0100694	$T^{0.5}$
−0.00183098	T
$1.26994\ 10^{-5}$	T^2
$-8.78171\ 10^{-5}$	T^3
$4.91795\ 10^{-6}$	m^2T^2
$-7.52939\ 10^{-8}$	T m
$-4.9594\ 10^{-8}$	m^2T
$-4.19861\ 10^{-8}$	m^3T
$9.60198\ 10^{-7}$	m T^2
$1.27846\ 10^{-9}$	m T^3

factor, f^S, is closely approximated by (e.g., Heinrich and Seward, 1990):

$$f^S = \frac{1000 + W_{LiCl} m_{LiCl}}{1000 \cdot \rho_{LiCl}(m_{LiCl}, T)} \quad (1)$$

where W_{LiCl} is the molecular mass of LiCl. A power series equation was used to describe the density of the LiCl aqueous solution, $\rho_{LiCl}(m_{LiCl}, T)$, for LiCl molalities (m_{LiCl}) between 0.1 m and 20 m LiCl, and temperatures (T) between 5°C and 100°C. The coefficients (Table 2) were fitted by least squares methods to experimental data of Bogatykh and Evnovitch (1965), Gates and Wood (1985), Isono (1984), Jones and Bradshaw (1932), Lengyel et al. (1964), Millero et al. (1977), Ostroff et al. (1969), Out and Los (1980) and Suhrmann and Wiedersich (1953).

3. RESULTS AND INTERPRETATION

3.1. Description of the Electronic Spectra of Cu(II) Chlorides

The spectrophotometric data for solutions with systematically increasing Cl concentrations obtained at 25 and 90°C are presented in Figure 1. Vis-NIR spectral regions exhibit a broad, asymmetric band, corresponding to *d-d* electronic transitions at the Cu(II) centre (e.g., Hatfield et al., 1965). The absorbance increases and the band shifts to lower wavenumbers (i.e., lower energies) with increasing Cl concentration (Fig. 1a). This change is consistent with the successive replacement of water ligands by weaker field chloride ligands (spectrochemical series; e.g., Shriver et al., 1996). The bands in the UV-Vis region (Fig. 1c,d) are attributed to charge transfer transitions between Cu(II) centres and surrounding ligands (e.g., Furlani and Morpurgo, 1963; Hatfield et al., 1965). The spectral features in the UV-Vis region are much more distinctive than those in the Vis-NIR region. At the lowest chloride concentration (Cl_{tot}=0.0048 m), the spectrum shows only a weak absorbance in the far UV region (Fig. 1d, spectrum 1). As the chloride concentration increases, a band develops at ~39800 cm^{-1} (Fig. 1d, arrow 2). Above approximately 1 m LiCl, this band increases rapidly in intensity and red shifts by approximately 3000 cm^{-1} with increasing LiCl concentration (Fig. 1d, arrow 3). Above ~2.5 m LiCl, a new absorption band appears at 25700 cm^{-1} (Fig. 1; arrow 4a); the growth of this band causes a change in the colour of the solutions from a faint blue at lower LiCl molalities to a yellow colour in solutions with higher LiCl

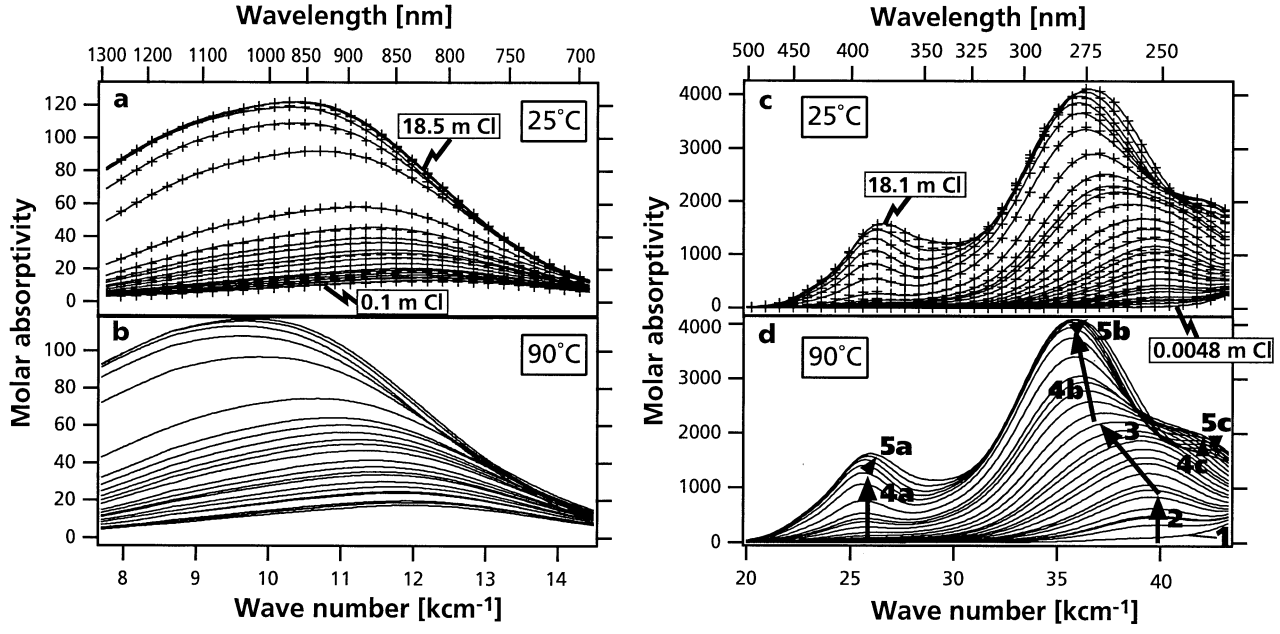

Fig. 1. Electronic spectra of Cu(II) in acidic LiCl solutions at 25 and 90°C. (**a** and **b**) Vis-NIR range, (**c** and **d**) UV-Vis range. The crosses in **a** and **c** are the calculated spectra for the 5-species model. The solution compositions are listed in Table 1. The arrows and labels 1 to 5 in Figure 1d show the 5 different trends in the spectral changes with increasing Cl-concentrations, that are interpreted as indicating the presence of at least 5 different Cu(II) complexes in the experiment.

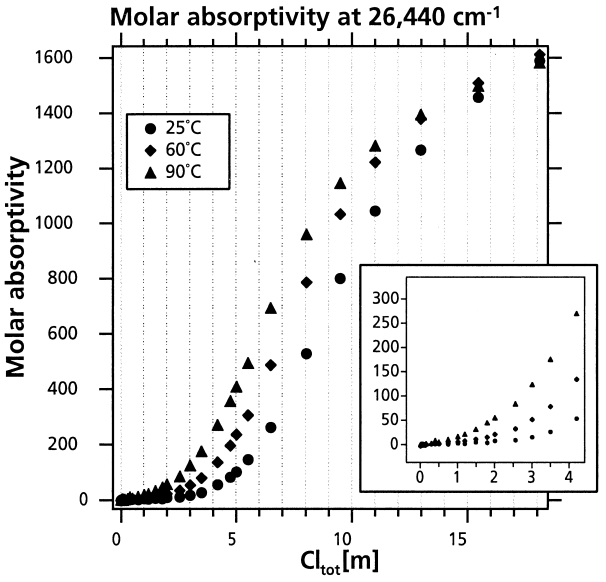

Fig. 2. Absorbance change at 26440 cm^{-1} as a function of chlorinity and temperature. 26440 cm^{-1} is the energy corresponding to the maximum absorbance in the near-VIS range at 18.1 m LiCl.

molalities. In parallel, another band appears at ~42900 cm^{-1} as a shoulder on the main band (Fig. 1; arrow 4c). The main band continues to grow and to shift towards lower energies (Fig. 1; arrow 4b). Above 10 m LiCl, the intensity of the band at 42900 cm^{-1} starts to decrease, and the remaining two bands shift towards higher wavenumbers by ~400 cm^{-1} (Fig. 1; arrows 5a,b,c), with only a slight increase in intensity.

Increasing temperature from 25°C to 90°C has only small effects on the absorbance spectra. The shape of the spectra and the molar absorbance do not change between the two temperatures; however, there is a small difference in the band in the UV-Vis at approximately 26000 cm^{-1}. That band starts increasing in intensity with lower LiCl concentration at 90°C than at 25°C (Fig. 2).

Qualitatively it is difficult to discern how many complexes are necessary to describe the changes in the Vis-NIR spectra; however, based on how absorbance changes at individual wavelengths there appears to be a minimum of 3 or 4 complexes. The changes in the UV-Vis spectra are more distinct, where it appears a minimum of 5 complexes are necessary to describe the spectra (see arrows in Fig. 1d). Quantitative interpretation of the spectra is necessary to estimate the molar absorbance spectra and fractions of individual complexes and derive their thermodynamic properties.

3.2. Interpretation of Spectra

The quantitative interpretation of spectra can be difficult, especially in our case where spectra for individual complexes overlap. First we review briefly the principles involved in interpreting absorbance spectra numerically and then follow with the detailed description of how we interpreted our experimental data.

3.2.1. Background principles

According to the Beer-Lambert law, the absorbance, A^S_λ, measured at wavelength λ in solution S is a function of the path-length l_{path}, the molar concentrations M^S_n of each of the absorbing complexes n (NAS = total number of absorbing species) in the solution S and the molar absorptivity coefficient $\varepsilon_{n,\lambda}$ at wavelength λ (e.g., Alpert, 1973):

$$A^S_\lambda = 1_{path} \sum_{n=1}^{NAS} M^S_n \epsilon_{n,\lambda} \quad (2)$$

The Beer-Lambert law is based on the molarity scale, but geochemists often use the molality scale (e.g., "standard thermodynamic convention" stated in Anderson and Crerar, 1993). Using the molar to molal conversion factor for solution S, f^S [Eqn. 1], Eqn. 2 can be rewritten:

$$\tilde{A}^S_\lambda = \frac{f^S \cdot A^S_\lambda}{1_{path}} = \sum_{n=1}^{NAS} m^S_n \epsilon_{n,\lambda} \quad (3)$$

where m^S_n is the molal concentration of complex n in solution S. To study stepwise ligand substitution, series of spectra are measured under similar conditions (e.g., constant Cu concentration, temperature, pH), but with varying concentrations of the ligand. The resulting absorbance data can be cast in a matrix $\tilde{\mathbf{A}}$ of total absorbances, where each column represents a particular wavelength, and each row represents a solution with a different ligand concentration. Using matrix notation, the Beer-Lambert law is written as:

$$\tilde{\mathbf{A}} = \mathbf{C} * \mathbf{E} \quad (4)$$

where $\mathbf{C}$ (number of solutions $\times$ NAS) is the matrix of concentrations of the absorbing species, and $\mathbf{E}$ (NAS $\times$ number of sampled wavelengths) is the matrix of molar absorptivity coefficients. The goal of the quantitative interpretation of spectroscopic data is to calculate the concentration and molar absorptivity of individual species in solutions that contain mixtures of absorbing species, i.e., to find the matrices $\mathbf{C}$ and $\mathbf{E}$ that best reproduce the experimental data. At first sight, this is a simple linear algebra problem. There is a fundamental problem, however, in that an infinite number of solutions can be derived using linear algebra, but there is only one physically correct solution (e.g., Tauler and Casassas, 1989). The correct solution ($\mathbf{C} * \mathbf{E}$) is related to any other solution ($\mathbf{D} * \mathbf{F}$) by a rotation $\mathbf{R}$ ($\mathbf{R}$ is an orthogonal, square matrix and $\mathbf{R}^T$ is its transpose), or by a scalar multiplication factor k:

$$\tilde{\mathbf{A}} = \mathbf{D} * \mathbf{F} = (\mathbf{C}\ \ \mathbf{R}) * (\mathbf{R}^T * \mathbf{E}) = \mathbf{C} * \mathbf{E} \quad \text{(rotational ambiguity)} \quad (5)$$

$$\tilde{\mathbf{A}} = \mathbf{D} * \mathbf{F} = (k\mathbf{C}) * (1/k\ \mathbf{E}) = \mathbf{C} * \mathbf{E} \quad \text{(scaling ambiguity)} \quad (6)$$

These ambiguities can be resolved if "pure variables," i.e., wavelengths where only one complex absorbs, are available (Malinowski, 1977). Pure variables are rarely present in UV-Vis-NIR spectra, which commonly display broad, overlapping bands (e.g., Susak and Crerar, 1984). In such cases, one must

rely on physical and/or chemical constraints that are applied during a least-squares minimisation to obtain the physically and chemically relevant solution.

Two families of algorithms for data interpretation can be distinguished, based on the type of constraints applied in the interpretation. The first family, originally implemented in the program SQUAD (Legget, 1977, Legget and McBryde, 1975), uses the constraint of a non-linear thermodynamic speciation model. A non-linear least-squares method is used to optimise the molar absorptivity coefficients and the equilibrium constants of formation of the absorbing species. SQUAD has been used successfully in geochemical studies (e.g., Heinrich and Seward, 1990, Bebie et al., 1998). The method used in the other family of algorithms, subsequently referred to as "model-free" method (e.g., Tauler and Casassas, 1989), does not require any assumption on the chemistry of the system, other than the number of absorbing complexes present. In particular, the "model-free" method requires no assumption about the nature of the absorbing complexes (e.g., stoichiometry) or a thermodynamic model. The physically relevant solution is retrieved using constraints such as non-negativity for concentrations and molar absorptivities, closure (sum of the concentrations of some species = known quantity) and unimodality (only one maximum in the concentration profiles; De Juan et al., 1997; Gampp et al., 1985; Saurina et al., 1995; Tauler and Casassas, 1989; 1992). The "model-free" method allows the determination of the molar absorptivity coefficients and concentrations of each absorbing complex in the experimental solutions.

3.2.2. Preliminary Data Analysis

The molar absorbance data were interpreted quantitatively in several steps:

1. Estimate the number of factors, i.e., contributing aqueous complexes, necessary to describe the absorbance data, using principal component analysis (PCA; e.g., Malinowski and Howery, 1980).
2. Fit spectra and fractions of individual complexes to the absorbance data using "model-free" analysis and the number of factors estimated by PCA. The computer code implementing an "alternating least squares" method was supplied by Anna de Juan (De Juan et al., 1997, De Juan and Tauler, 1999). The results are used to elucidate the geometry and stoichiometry of the complexes and to provide initial estimates for thermodynamic properties to be fitted to the spectra.
3. Set up a thermodynamic model, including activity coefficient estimates, and fit the molar absorbance spectra and logarithms of formation constants for Cu(II)-chloride aqueous complexes.
4. Study the stability of the numerical solution and estimate the uncertainties on fitted values of the thermodynamic properties.

PCA indicates that a minimum of 4 factors (corresponding to 4 aqueous complexes) is necessary to describe the NIR-Vis spectra (Fig. 3b), whereas a minimum of 5 factors is necessary to describe the UV-Vis spectra (Fig. 3a). The latter is consistent with the qualitative interpretation of the UV-Vis spectra (Fig. 1d). The residual calculated for 5 factors is still approximately

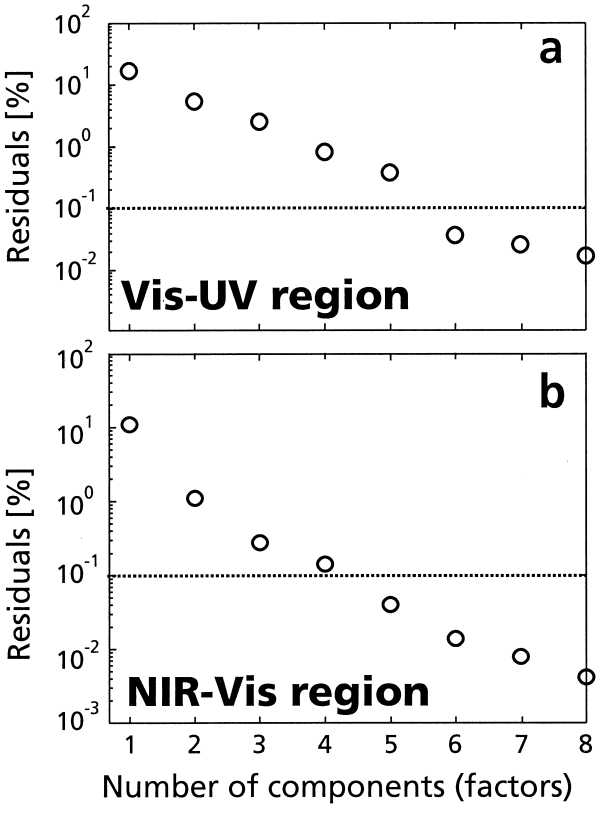

Fig. 3. Principal component analysis of the spectroscopic data at 25°C (**a**) for UV-Vis spectra, (**b**) for Vis-NIR spectra. Residual are calculated as $100\sqrt{\frac{(x_i - x)^2}{x_i^2}}$, x_i is the observed value, and x the model value. The dashed line represents a minimum experimental error.

3 times the analytical precision. It is, therefore, possible that a sixth factor is necessary to explain the UV-Vis data, although the calculated residual for 6 factors is less than the analytical precision. It is unlikely that there are more than 6 complexes contributing to the UV-Vis spectrum, as the calculated residuals for higher factor models are less than the analytical precision and do not decrease markedly between 6, 7 and 8 factor models.

In the "model-free" analysis, we assumed positive molar absorptivity coefficients and concentrations (i.e., non-negativity constraint) and the sum of the concentrations of all absorbing complexes = total copper concentration (i.e., closure constraint). The absorptivity coefficients for $[Cu]^{2+}_{aq}$ were fixed using the spectra recorded for the lowest chloride concentration. Analysis of the data with and without the unimodality constraint, however, only changed the calculated concentrations for Cu(II)-complexes by a maximum of 10%. In the final "model-free" analysis the unimodality constraint was included because this prevented complexes (e.g., $[CuCl]^{+}_{aq}$) that are present at lower chloride concentrations from reappearing at the highest chloride concentrations.

The "model-free" analysis is consistent with the qualitative and quantitative interpretation that a minimum of 5 complexes is necessary to explain UV-Vis spectra (Fig. 4). Fits with 4 complexes were very poor (residuals $>>$ 0.1%). Fits with 6 complexes are sensitive to initial guesses and applied con-

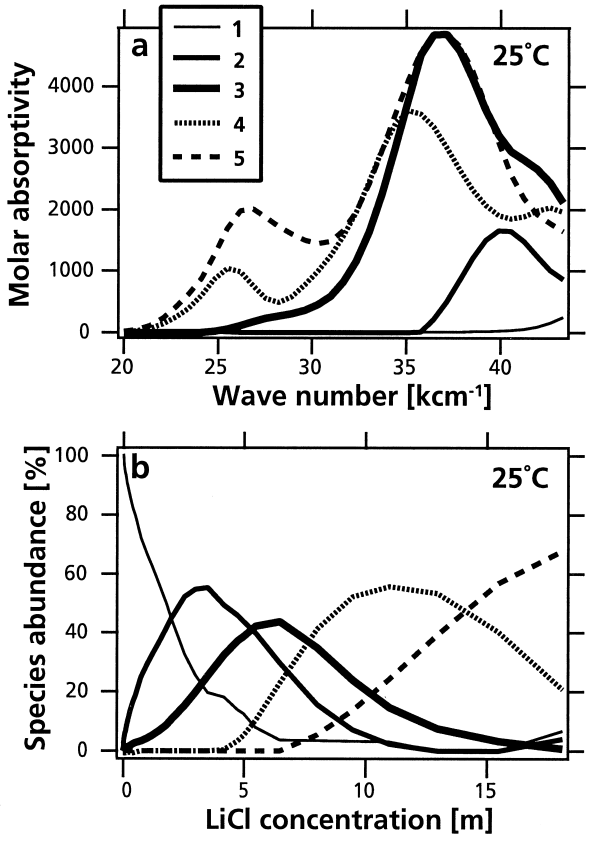

Fig. 4. Results of the "model-free" analysis of the spectroscopic data. (**a**) spectra of the 5 individual species; (**b**) distribution of the 5 species as a function of LiCl concentration. The species are numbered 1 to 5, as the "model-free" analysis does not require any assumption on their nature.

straints, and generally led to unrealistic concentration profiles or absorbance spectra for individual species.

3.2.3. Development of a Thermodynamic Model

Deriving thermodynamic properties from the absorbance spectra requires a model that accounts for the properties (i.e., log K of formation reactions) and activity coefficients of all the relevant aqueous species, including non-copper species such as those containing lithium and chloride.

The Cu(II) complexes to be considered are of the type $[Cu^{II}Cl_n]^{2-n}_{aq}$. Throughout this paper, we use the subscript "aq" to refer to a general stoichiometry where we do not explicitly account for H_2O ligands in the first coordination shell. In the absence of "aq," we specify the geometry of the species. For example, $[CuCl_4]^{2-}_{aq}$ can refer to $[CuCl_4]^{2-}$ (tetrahedral), $[CuCl_4]^{2-}$ (square pyramidal), or $[CuCl_4(OH_2)_2]^{2-}$ (octahedral). We checked for the existence of polynuclear Cu complexes, as they have been identified in studies of related systems (e.g., Cu(I)-bisulphide complexes; Helz et al., 1993; Thompson and Helz, 1994), by measuring the Vis-NIR absorbance spectra of acidified 1 m NaCl solutions containing a range of dissolved $CuSO_4$ concentrations (0.0016 m to 0.08 m). A change in copper speciation reflecting the presence of polynuclear complexes should become evident as changes in band shape (e.g., Smith, 1976) and/or non-linear changes in absorbance with increasing $CuSO_4$ concentration. Neither was observed, indicating no change in copper speciation in 1 m NaCl solutions containing up to at least 0.08 m Cu. Subsequent experiments contained less than 10^{-3} m Cu, well below the concentrations in the test experiments.

The other chemical species considered in the model are $[H]^+_{aq}$, $[HCl]^0_{aq}$, $[Li]^+_{aq}$, $[Cl]^-_{aq}$ and $[LiCl]^0_{aq}$. Hydroxy-species such as $[OH]^-_{aq}$ and $[LiOH]^0_{aq}$ are not included in our model because their concentration was negligible under our experimental conditions (pH $<$ 4). H_2O is not included in the model because we choose not to include waters of hydration in the reactions of formation of the copper complexes; therefore, H_2O is not involved in our model reactions. Polynuclear ion pairs with Li and Cl probably exist, based on the presence of such complexes in the NaCl and KCl systems (e.g., Oelkers and Helgeson, 1993; Pokrovskii and Helgeson, 1997). Molecular dynamic modelling of NaCl solutions suggests that different polynuclear clusters (ion pairs) exist in strong electrolyte solutions, even at moderate salt concentrations (Driesner et al., 1998), where according to their calculations, $[Na_2Cl]^+_{aq}$, $[NaCl_2]^-_{aq}$, and $[Na_2Cl_2]^0_{aq}$ account for 20.4% of the ions in 1 m NaCl solution at 25°C. At supercritical temperatures (380°C), the free ions Na^+ and Cl^- account only for 12.8% of the ions, and clusters as large as $[Na_4Cl_4]^0_{aq}$ were predicted. It is difficult to use these types of complexes in a thermodynamic model, due to their large number and lack of experimental or theoretical studies on their role in highly concentrated brines (>1 molal). A simple model, that does not account explicitly for polynuclear Li-Cl species is applied to this study. This affects the calculation of the true ionic strength ($\bar{I}$), and hence the activity coefficients used in this study; however, more complete models cannot be developed until we have a better understanding of the structure and properties of highly concentrated electrolyte solutions.

The concentrations and activities of each species can be obtained by solving a system of mass action equations, mass balance equations, and an equation for electrical neutrality (e.g., Anderson and Crerar, 1993, pp. 505–507). The mass action equations are:

$$\text{Formation of } [HCl]^0_{aq}: \quad K_{[HCl]^0_{aq}} = \frac{m_{[HCl]^0_{aq}}\bar{\gamma}_{[HCl]^0_{aq}}}{m_{[H]^+_{aq}} m_{[Cl]^-_{aq}} \bar{\gamma}_{[H]^+_{za}} \bar{\gamma}_{[Cl]^-_{aq}}} \tag{7}$$

$$\text{Formation of } [LiCl]^0_{aq}: \quad K_{[LiCl]^0_{aq}} = \frac{m_{[LiCl]^0_{aq}}\bar{\gamma}_{[LiCl]^0_{aq}}}{m_{[Li]^+_{aq}} m_{[Cl]^-_{aq}} \bar{\gamma}_{[Cl]^-_{aq}} \bar{\gamma}_{[Li]^+_{aq}}} \tag{8}$$

Formation of Cu(II) chloro-complexes:

$$K_n = \frac{m_{[CuCl_n]^{2-n}_{aq}}\bar{\gamma}_{[CuCl_n]^{2-n}_{aq}}}{m_{[Cu]^{2+}_{aq}} \bar{\gamma}_{[Cu]^{2+}_{aq}} (m_{[Cl]^-_{aq}} \bar{\gamma}_{[Cl]^-_{aq}})^n}, \tag{9}$$

where n represents the number of chloride ligands and $\bar{\gamma}$ are the activity coefficients for the subscripted individual complexes. There are three mass balance equations:

$$m_{Cu_{tot}} = \sum_n m_{[CuCl_n]^{2-n}_{aq}}, \tag{10}$$

$$m_{Cl_{tot}} = m_{[HCl]^0_{aq}} + m_{[LiCl]^0_{aq}} + m_{[Cl]^-_{aq}} + \sum_n n \cdot m_{[CuCl_i]^{2-i}_{aq}}, \quad (11)$$

$$m_{Li_{tot}} = m_{[LiCl]^0_{aq}} + m_{[Li]^+_{aq}} \quad (12)$$

Activity coefficients vary as a function of ionic strength, properties of the solvent and dissolved species, temperature and pressure. Two types of models are widely used: ion-interaction and ion-pairing (e.g., Anderson and Crerar, 1993). The ion-interaction model, as formulated by Pitzer (1973), does not account explicitly for ion association (including complex formation), and describes the properties of a solution in term of interactions between free ions. This approach has been particularly successful in predicting mineral solubilities in concentrated electrolyte solutions (e.g., Harvie et al., 1984), but does not allow for extrapolations outside the range of available experimental data (e.g., see discussion in Anderson and Crerar, 1993, p 463–465). The second type of model, ion-pairing, accounts explicitly for all species present in the aqueous solution. This approach is well suited for the modelling of trace amounts of metal ions that form stable complexes (e.g., Helgeson et al., 1981), and has been developed to allow the extension of the model to pressures and temperatures outside the range where experimental data are available (Helgeson and Kirkham, 1974a; 1974b; Helgeson et al., 1981). Millero and Hawke (1992) and Millero et al. (1995) combined the ion-interaction and ion-pairing models, the former being used to describe the ionic interaction between the main constituents of sea-water, and the latter accounting for the strong interaction between the trace metal cations and the major anions.

In this study the Helgeson and Kirkham (1974b) approach is used to estimate activity coefficients over the ion-interaction and combined models because it is well suited for calculating activities of trace element complexes in concentrated salt solutions, i.e., Cu(II)-chloride complexes in LiCl solutions. Moreover, we found that it could describe the existing experimental data with only a small modification. Initially, individual activity coefficients for major and minor charged species were calculated using the "b-dot" equation, a version of the Debye-Hückel equation extended with a linear term in ionic strength (Helgeson and Kirkham, 1974b):

$$\log(\bar{\gamma}) = -\frac{A_\gamma z_n^2 \bar{I}^{1/2}}{1 + B_\gamma \mathring{a}_n \bar{I}^{1/2}} + b_{\gamma,LiCl}\bar{I} + \Gamma_\gamma, \quad \text{where } \bar{I} = 1/2 \sum_i m_i z_i^2 \quad (13)$$

A_γ and B_γ are the Debye-Hückel solvent parameters taken from Tables 1 and 2 in Helgeson and Kirkham (1974b), and $b_{\gamma,LiCl}$ is a temperature-dependent interaction parameter for LiCl-dominated aqueous solutions (see below). $\mathring{a}_n$ is the distance of closest approach for ion n, and is given a value of 5.0 Å for divalent and trivalent ions, and 4.0 Å for monovalent ions with the exception of the proton H^+ which was attributed a value of 9.0 Å (e.g., Kielland, 1937). $\bar{I}$ is the effective (or true) ionic strength, and m_i and z_i denote the molality and charge of the i^{th} aqueous species, respectively. Γ_γ is a mole fraction to molality conversion factor, given by $\Gamma_\gamma = -\log(1+0.18053m^*)$, where m* refers to the sum of the molalities of all solute species.

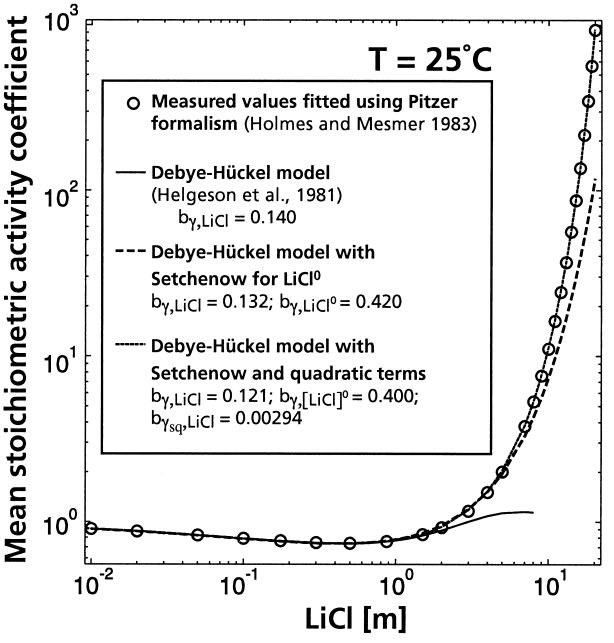

Fig. 5. Comparison between the mean stoichiometric activity coefficient of LiCl solutions obtained using the Pitzer parameters fitted by Holmes and Mesmer, 1983, with those predicted using the Debye-Hückel model with parameters fitted by Helgeson et al. (1981), and with the parameters derived in the present study. The circles (Pitzer model) closely match the available experimental data.

The relation between the stoichiometric ($\gamma_{[Cl]^-_{aq}}$, no ion-pairing) and ionic ($\bar{\gamma}_{[Cl]^-_{aq}}$, with ion-pairing) activity coefficients is (e.g., Eqn. 5 in Millero and Hawke, 1992):

$$a_{[Cl]^-_{aq}} = \gamma_{[Cl]^-_{aq}} m^{tot}_{LiCl} = \bar{\gamma}_{[Cl]^-_{aq}} m_{[Cl]^-_{aq}} \quad (14)$$

Because the distances of closest approach are assumed equal for monovalent species, and using the definition of the mean stoichiometric activity coefficient (Eqn. 57 in Helgeson et al., 1981), we have:

$$\gamma_{\pm,LiCl} = (\gamma_{[Cl]^-_{aq}}\gamma_{[Li]^+_{aq}})^{1/2} = \gamma_{[Cl]^-_{aq}} \quad (15)$$

Thus, for a LiCl solution in which the ion pair $[LiCl]^0_{aq}$ is taken into account the mean stoichiometric activity coefficient is given by:

$$\gamma_{\pm,LiCl} = \frac{m^{tot}_{LiCl} - m_{[LiCl]^0_{aq}}}{m^{tot}_{LiCl}} \bar{\gamma}_{[Cl]^-_{aq}} \quad (16)$$

Using existing values for A, B, $\mathring{a}_n$, and values for $b_{\gamma,LiCl}$ taken from Helgeson et al. (1981; Table 26), the dissociation constant for $LiCl^0$ calculated with SUPCRT (Johnson et al., 1992), and assuming the activity coefficients of neutral species are equal to one, the b-dot equation reproduces accurately the experimental mean stoichiometric activity coefficients of LiCl up to approximately 1 m LiCl (Fig. 5). At greater LiCl concentrations, the predicted values are less than the measured values and diverge with increasing LiCl concentration (Fig. 5). To fit the entire range of LiCl concentration for which experimental data are

Table 3. Debye-Hückel parameters ($b_{\gamma,LiCl}$), Sétchenow coefficient ($b_{\gamma,[LiCl]^0_{aq}}$), and dissociation constants for $[LiCl]^0_{aq}$ ($\log K_d^{[LiCl]^0_{aq}}$) used in this study. The dissociation constants of $[HCl]^0_{aq}$ used in this study are also given.

	This Study			Helgeson et al. (1981)	SUPCRT92	
Temp [°C]	$b_{\gamma,LiCl}$	$b_{\gamma,[LiCl]^0_{aq}}$	$b_{\gamma_{sq},LiCl}\cdot 10^3$	$b_{\gamma,LiCl}$	$\log K_d^{[LiCl]^0_{aq}}$	$\log K_d^{[HCl]^0_{aq}}$
25	0.121	0.400	2.94	0.140	1.511	0.711
60	0.113	0.675	1.90	0.131	1.382	0.803
90	0.109	0.336	1.16	0.123	1.235	0.774

available, the b-dot equation has been extended by adding a quadratic term:

$$\log(\bar{\gamma}) = -\frac{A_\gamma z_n^{21/2}}{1 + B_\gamma \mathring{a}_n \bar{I}^{1/2}} + b_{\gamma,LiCl}\bar{I} + b_{\gamma_{sq},LiCl}\bar{I}^2 + \Gamma_\gamma, \quad (17)$$

and estimating the activity coefficient for the neutral species, $[LiCl]^0_{aq}$, with the Setchénow equation (Setchénow, 1889):

$$\log(\bar{\gamma}_{[LiCl]^0_{aq}}) = b_{\gamma,[LiCl]^0_{aq}} I + \Gamma_\gamma \quad (18)$$

Alternative extensions to the b-dot equation all failed to fit the available data well over the entire concentration range. We tried three alternatives:

1. An initial b-dot term of $\bar{I}^2$;
2. An exponential term instead of the quadratic b-dot term;
3. A Setchénow coefficient but no quadratic term.

Values of the b-dot coefficient, $b_{\gamma,LiCl}$, Setchénow coefficient, $b_{\gamma,[LiCl]^0_{aq}}$, and the extended quadratic coefficient, $b_{\gamma_{sq},LiCl}$ were fitted to the mean ionic activity coefficients for LiCl (Holmes and Mesmer, 1983) following the procedure of Pokrovskii and Helgeson (1997), and are listed in Table 3. This model fits the experimental data within 1% and represents the mean ionic activity coefficient of a LiCl solution over the whole range of concentrations used in our experiments (Fig. 5). The new values of the b-dot coefficient ($b_{\gamma,LiCl}$; Table 3) are close to those tabulated by Helgeson and Kirkham (1974b). Direct comparisons of our values for the Setchénow coefficient, $b_{\gamma,[LiCl]^0_{aq}}$, are not possible because of a lack of published values; however, they are within the range of the values reported for another 1:1 salt, KCl ($0.112 < b_{\gamma,[KCl]^0_{aq}} < 1.09$ between temperatures of 100°C and 325°C (Pokrovskii and Helgeson, 1997).

$[HCl]^0_{aq}$ is also included in our thermodynamic model and we assumed its activity to be one (i.e., Setchnénow coefficient $b_{\gamma,[HCl]^0_{aq}} = 0$). It is unnecessary to use a more sophisticated estimate because $[HCl]^0_{aq}$ is only a minor species in our experiments and accurate calculated pH values are not required to interpret our data. The influence of a non-zero Sétchenow coefficient for another neutral complex, $[CuCl_2]^0_{aq}$, is discussed in the quantitative interpretation sections below.

3.2.4. Procedure for the fitting of log k

In fitting the data, a matrix of molar absorptivity coefficients **E** and a set of the logarithms equilibrium constants (log K) are required that minimise the residuals **u** in Eqn. 19:

$$\tilde{\mathbf{A}} = \mathbf{C} * \mathbf{E} + \mathbf{u} \quad (19)$$

Solving Eqn. 19 by using a least squares method is equivalent to finding a minimum for the objective function χ^2:

$$n\chi^2 = \sum_n \mathbf{u}^T\mathbf{u} = \sum_n [(\tilde{\mathbf{A}} - \mathbf{C}\,\mathbf{E})^T(\tilde{\mathbf{A}} - \mathbf{C}\,\mathbf{E})] = \sum_n (\tilde{\mathbf{A}}^T\tilde{\mathbf{A}} - 2\tilde{\mathbf{A}}^T\mathbf{C}\,\mathbf{E} + \mathbf{E}^T\mathbf{C}^T\mathbf{C}) \quad (20)$$

where Σ represents the sum of the n elements in the vector of squared residuals. The optimisation of the equilibrium constants and molar absorptivity coefficients is based on two optimisation algorithms performed in outer and inner programming loops. Within the inner loop, Eqn. 19 is solved for **E** for a given set of equilibrium constants (K) and with non-negativity constraints on the elements of **E**. A quadratic programming method was used that usually finds the absolute minimum (Neumaier, 1998). The matrix of concentrations (**C**) is calculated by a distribution of species calculation using a customised version of EQBRM (Anderson and Crerar, 1993). Then, in the outer loop, the values of K are varied using a Nelder-Mead type simplex algorithm (Nelder and Mead, 1965) until a local minimum for χ^2 is obtained.

In the fitting, a subset of 35 absorbance values per spectra, equally distributed on the energy scale between 20000 and 43300 cm^{-1} (500–230 nm) were used in the UV-Vis, and between 8980 and 15000 cm^{-1} (666–1300 nm) in the Vis-NIR. This number of data points provides sufficient coverage given the broad nature (width) of the absorption bands (Fig. 1). Fits using different subsets of 35 data points per spectra and larger subsets (up to 80 points per spectrum) resulted in log K values within 0.02 absorbance unit corresponding to differences that are well within our estimated uncertainties (see below).

3.2.5. Choice of speciation models

The choice of copper complexes to include in our thermodynamic model is non-trivial because the stereochemistry of copper(II) ($[Ar]3d^9$) complexes is very diverse. In particular Cu(II) complexes exhibit a strong Jahn-Teller distortion, which in the case of chloro-complexes contributes to a plethora of geometric arrangements of the ligands around the central atom (e.g., Smith, 1976). To rationalise the choice of a speciation model (i.e., number and type of copper-chloride complexes) that is consistent with our spectrophotometric data, a brief review is provided of the coordination chemistry of Cu(II) and information about the structure of Cu(II)-bearing aqueous solutions from Extended X-ray Absorption Fine Structure (EXAFS) data.

The Jahn-Teller distortion of Cu(II)-chloro-complexes is

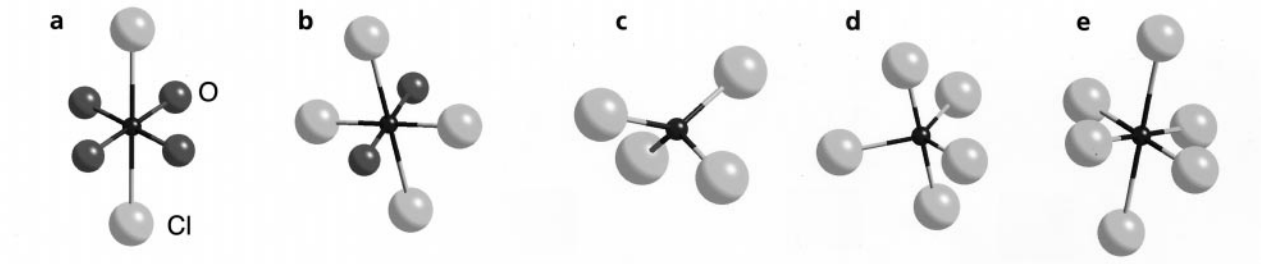

	Chloroxiphite $Pb_3CuO_2Cl_2(OH)_{2(s)}$ face-sharing octahedral chains	Eriochalcite $CuCl_2.2H_2O_{(s)}$ edge-sharing octahedral chains	$Cs_2[CuCl]_{4(s)}$ isolated distorted tetrahedra	$[Cr(NH_3)_6][CuCl]_{5(s)}$ isolated trigonal bipyramids	Tolbachite $CuCl_{2(s)}$ edge-sharing octahedral layers
Cu-O [Å]	1.982 (2x) 1.995 (2x)	2.010 (2x)			
Cu-Cl [Å]	2.966 (2x)	2.302 (2x) 2.983 (2x)	2.221 (2x) 2.235 (1x) 2.244 (1x)	2.314 (2x) 2.362 (3x)	2.262 (4x) 2.963 (2x)
Point group	D_{4h}	C_{2h}	D_{2d}	D_{3h}	D_{4h}

Fig. 6. Examples of the chloride coordination to Cu(II) in crystals. (**a**) chloroxiphite, (Finney et al., 1977); (**b**) eriochalcite (Harker, 1936); (**c**) Cs_2CuCl_4 (McGinnety, 1972); (**d**) $Cr(NH_3)_6CuCl_5$ (Raymond et al., 1968); (**e**) tolbachite (Burns and Hawthorne, 1993).

well illustrated by the mineral tolbachite, in which each Cu(II) ion is surrounded by 4 Cl^- ions at 2.262 Å and 2 Cl^- ion at 2.963 Å (D_{4h}; Fig. 6; Burns and Hawthorne, 1993). As might be anticipated from the weak ligand field provided by the chloride ligands, in mixed ligand complexes (e.g., Cl^- and H_2O) the Cl^- ligands are generally located along the long axis of a distorted octahedron (D_{4h}) in 6-coordinated Cu(II) chloro-complexes occurring in minerals, (e.g., $[CuCl_2(OH)_4]^{4-}_{(s)}$ in chloroxiphite, Finney et al., 1977; $[CuCl_4(OH_2)_2]^{4-}_{(s)}$ in eriochalcite, Harker, 1936; Figure 6). Distorted tetrahedral (D_{2d}) and trigonal bi-pyramidal geometries (D_{3h}) are also observed in solids (McGinnety, 1972; Raymond et al., 1968; Fig. 6).

EXAFS studies of Cu(II)-bearing solutions reveal that the hexa-aquo complex, $[Cu(OH_2)_6]^{2+}$, with distorted octahedral geometry (D_{4h}), is stable in pure water at room temperature (D'Angelo et al., 1997 and references therein). Experiments with solutions containing 3 m NaCl suggest that dissolved copper(II) centres exist in a distorted octahedral coordination, with an average of 1.0 ± 0.2 (1σ) Cl along the long axis at 2.85 ± 0.03 Å, and 1.0 ± 0.2 Cl in the equatorial plane at 2.29 ± 0.02 Å (D'Angelo et al., 1997). Collings et al. (2000), in their EXAFS study at higher chloride concentrations (up to 5.6 m NaCl) and higher temperature (up to 175°C), were not able to resolve the nature of the complexes (e.g., the axial ligands), but suggested the presence of $[CuCl_4]^{2-}_{aq}$ in 0.1 m $CuCl_2$ + 5.6 m NaCl solutions at 125°C.

Using existing evidence from EXAFS and electronic spectroscopy, we can interpret the geometry and stoichiometry of the Cu(II)-chloro-complexes from the spectra retrieved by the "model-free" analysis. The first complex present at the lowest concentrations of LiCl, is the distorted octahedral $[Cu(OH_2)_6]^{2+}$. The second and third complexes ($[CuCl]^+_{aq}$, $[CuCl_2]^0_{aq}$) are also distorted octahedral, based on EXAFS data (D'Angelo et al., 1997). The results of the "model-free" analysis indicate a major change in the UV-Vis spectral features of the higher-order Cu(II)-chloride complexes (Fig. 4). The change in the shape of the spectra of the third and fourth complexes can probably be attributed to a stereochemical change from distorted octahedral to distorted tetrahedral (e.g., Crerar et al., 1985). The UV-Vis spectrum of the fourth complex in the model-free analysis is very similar to the spectrum of distorted tetrahedral $[CuCl_4]^{2-}$ in $(C_2H_5NH_3)_2CuCl_{4(s)}$, with two major bands at 26400 and 35700 cm^{-1}, and a shoulder at ~42000 cm^{-1}. $[CuCl_4]^{2-}$ also occurs in solids with square planar geometry (D_{4h}; Desjardins et al., 1983). The synthesis of those compounds, however, requires water-free organic solvents, whereas distorted tetrahedral $[CuCl_4]^{2-}$-bearing compounds can be easily precipitated from aqueous solutions, and we thus favour the D_{2d} geometry (Fig. 6c). There is also a change in the shape of spectra between fourth and fifth complexes from the "model-free" analysis (i.e., disappearance of the band at ~43000 cm^{-1}; Fig. 4a). The UV-Vis spectrum of this last complex can be compared with the solid state spectra of $[CuCl_5]^{3-}$, which display two main bands at 27500 and 39000 cm^{-1} in $Cr(NH_3)_6CuCl_{5(s)}$ or 28400 and 35700 cm^{-1} in $dienH_3CuCl_{5(s)}$ (Allen and Hush, 1967). Again, the $CuCl_5^{3-}$ complex appears in different configuration with very similar energy, i.e., trigonal bipyramidal (D_{3h}; Raymond et al., 1968) and square pyramidal (e.g., Antolini et al., 1980), but the D_{3h} geometry is commonly observed in compounds crystallised from electrolyte solutions. Note that the distorted octahedral $[CuCl_6]^{4-}$ complex is unstable in aqueous solutions, as indicated by the rapid hydration of $[CuCl_6]^{4-}$ to $[CuCl_4(OH_2)_2]^{2-}$ in tolbachite in air (e.g., Burns and Hawthorne, 1993).

3.2.6. Results for alternative speciation models

In this study, the PCA discussed earlier suggests that five or six copper complexes are required to explain the data. Two

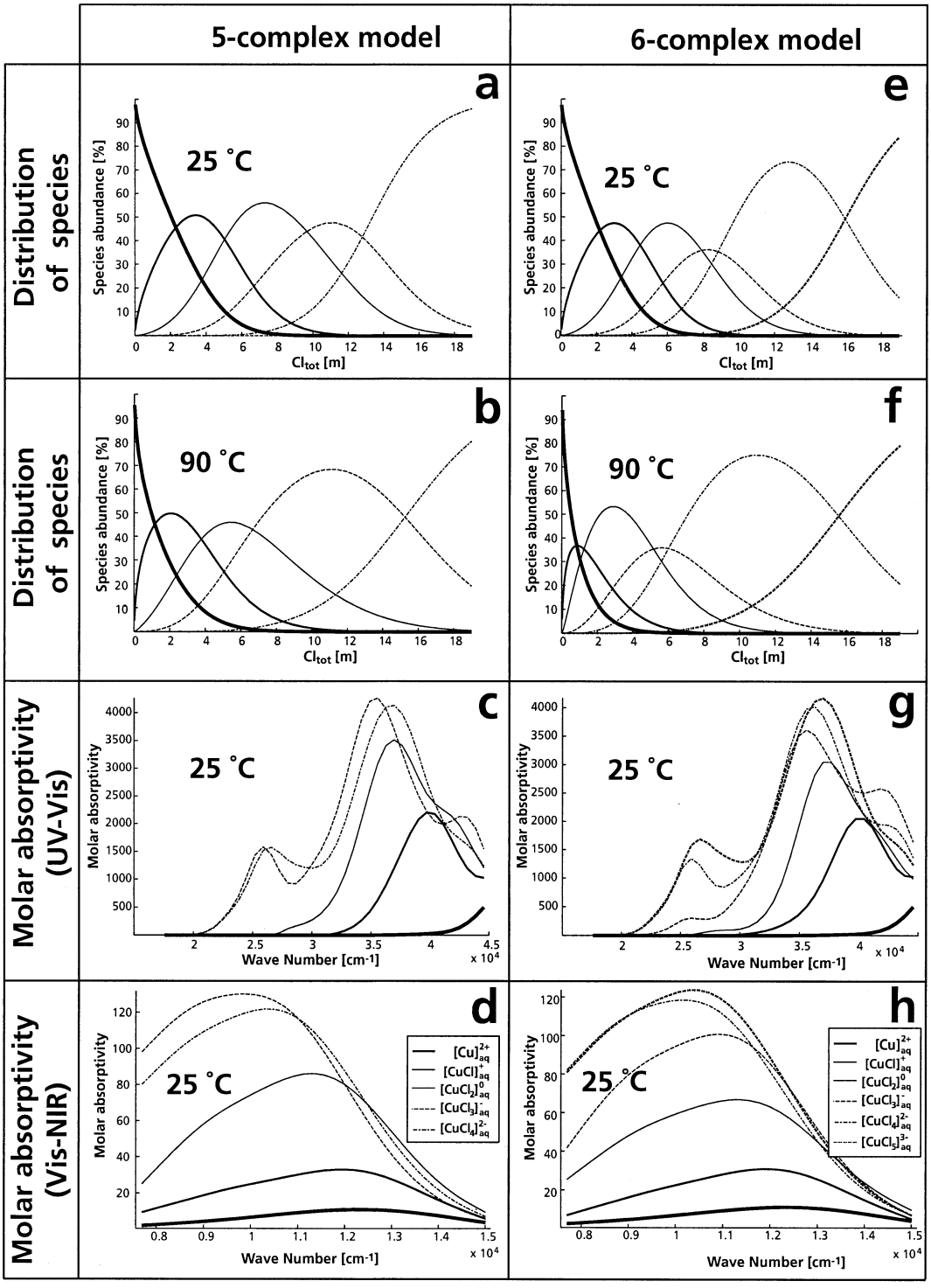

Fig. 7. Results from the quantitative interpretation of the spectroscopic data. (**a–d**) 5-complex model, (**e–h**) 6-complex model. (**c, g**) distribution of species at 25°C; (**a, e**) distribution of species at 90°C; (**c, g**) UV-Vis spectra of the individual species at 25°C; (**d, h**) Vis-NIR spectra of the individual species at 25°C.

alternative models were tested, one requiring 5 Cu(II) complexes, and the other 6. The fitted spectra of individual complexes and the calculated distributions of species for the five- and six-complex models are shown in Figure 7. We present comparisons between the results of our fits using the two models, as well as between our results and those of previous studies (Table 4). Additionally, the choice of the value for the activity of the neutral complex $[CuCl_2]^0_{aq}$, i.e., the value of the

Table 4. Values of log K (formation constants; equation (9)) of copper(II) complexes derived from the spectroscopic data in the UV-Vis region. Uncertainties at the 90% confidence level are given in parentheses.

Complex	Sverjensky et al. (1997)	Bjerrum (1987)	5-complex model	6-complex model
Temperature = 25°C				
$[CuCl]^{+}_{aq}$	0.40	~0	0.27 (−0.1/+0.2)	0.30 (−0.1/+0.1)
$[CuCl_2]^{0}_{aq}$	−0.69	~0.4	−0.63 (−0.1/+0.4)	−0.44 (−0.1/+0.1)
$[CuCl_3]^{-}_{aq}$	−2.29	~1.2	−2.44 (−0.3/+0.6)	−2.02 (−2.02/+0.5)
$[CuCl_4]^{2-}_{aq}$	−4.59	~2	−5.90 (−0.5/+1.0)	−4.39 (−0.1/+0.5)
$[CuCl_5]^{3-}_{aq}$	—	—	—	−9.0 (−0.1/+0.6)
Residuals	—	—	0.010	0.005
Temperature = 60°C				
$[CuCl]^{+}_{aq}$	0.50		0.53 (−0.1/+0.1)	0.51 (−0.2/+0.2)
$[CuCl_2]^{0}_{aq}$	−0.55		−0.13 (−0.3/+0.4)	0.36 (−0.6/+0.2)
$[CuCl_3]^{-}_{aq}$	−2.31		−1.75 (−0.5/+0.4)	−0.96 (−0.5/+0.5)
$[CuCl_4]^{2-}_{aq}$	−5.01		−5.1 (−1.0/+1.0)	−2.93 (−0.6/+0.5)
$[CuCl_5]^{3-}_{aq}$	—		—	−7.1 (−0.8/+0.7)
Residuals	—		0.010	0.005
Temperature = 90°C				
$[CuCl]^{+}_{aq}$	0.66		0.73 (−0.1/+0.1)	0.87 (−0.3/+0.2)
$[CuCl_2]^{0}_{aq}$	−0.28		0.36 (−0.3/+0.4)	1.19 (−0.8/+0.2)
$[CuCl_3]^{-}_{aq}$	−2.08		−1.04 (−0.5/+0.3)	0.00 (−1.0/+0.5)
$[CuCl_4]^{2-}_{aq}$	−5.00		−4.3 (−2.0/+1.0)	−1.80 (−0.9/+0.5)
$[CuCl_5]^{3-}_{aq}$	—		—	−5.9 (−0.9/+0.7)
Residuals	—		0.011	0.005

Setchénow coefficient (Eqn. 18), influences the results and is discussed using the 6-complex model as an example.

The fitted UV-Vis spectra and calculated distribution of species using a five-complex speciation model are shown in Figure 7a–d. The speciation model includes $[Cu]^{2+}_{aq}$, $[CuCl]^{+}_{aq}$, $[CuCl_2]^{0}_{aq}$, $[CuCl_3]^{-}_{aq}$ and $[CuCl_4]^{2-}_{aq}$, and is therefore similar to the models previously given in the literature for aqueous (e.g., Bjerrum, 1987) and organic solvents (e.g., Bentouhami et al., 1992; Djabi et al. 1994). The molar absorptivity spectra are similar to those given by the "model-free" analysis (Figs. 7c and 4a). Thus, as mentioned above, the first three complexes have distorted octahedral geometries. The fourth complex, $[CuCl_3]^{-}_{aq}$, is tetrahedrally coordinated. The fifth complex may also have a distorted tetrahedral geometry; however, the disappearance of the band at approximately 42000 cm^{-1} (Fig. 7b) may indicate another geometry, as this band is found in the solid state spectra of crystals containing the $[CuCl_4]^{2-}$ ion (Desjardins et al., 1983).

The fitted spectra and calculated distribution of species for the six-complex model are shown in Figure 7e–h. The speciation model includes the same complexes as for the five-complex model plus $[CuCl_5]^{3-}_{aq}$. As in the five-complex model, the first three complexes are octahedrally coordinated. In the six-complex model, the geometry of the $[CuCl_3]^{-}_{aq}$ complex may be either octahedral or tetrahedral, where the shape of the fitted spectrum for that complex is dependent on the choice of the Setchénow coefficient for $[CuCl_2]^{0}_{aq}$ (see below). The molar absorptivity spectra of the fifth and sixth complexes in the 6-complex model are similar to the spectra of the fourth and fifth complexes in the 5-complex model, respectively. Thus, based on the shape of its fitted spectrum, the $[CuCl_4]^{2-}_{aq}$ complex is tetrahedrally coordinated (Fig. 7g), and the possible copper-chloride complex at the highest LiCl concentration, $[CuCl_5]^{3-}_{aq}$, probably has bipyramidal trigonal geometry (D_{3h}).

The formation constants and residuals determined using the 5- and 6-complex models are presented in Table 4. These values are based on the regression of the spectroscopic data in the UV-Vis range. The residuals are smaller for the 6-complex model, but for the 5-complex model the residuals are within the estimated analytical error. There is no compelling reason to include the visible-NIR data in the fits; however, we tested the possibility by fitting the visible-NIR spectra using log K values in Table 4. The calculated residuals were less than 0.005 absorbance units, lower than the estimated analytical precision of 0.01 absorbance units, indicating that the Vis-NIR data are consistent with the UV-Vis data, and there is no additional information to be gained by including the Vis-NIR data. Nevertheless, the consistency in interpretations obtained across different types of electronic features and different Cu(II) concentrations gives confidence to the analytical methodology presented herein.

The activity coefficient for the neutral species, $[CuCl_2]^{0}_{aq}$, is unknown, but has an effect on the results of the fitting. Different values of the Setchénow coefficient, $b_{\gamma,[CuCl_2]^{0}_{aq}}$, were assumed to choose an optimal value. With $b_{\gamma,[CuCl_2]^{0}_{aq}} = 0$ (i.e., $\gamma_{[CuCl_2]^{0}_{aq}} = 1$), $[CuCl_3]^{-}_{aq}$ is calculated to be only a minor complex with absorptivity coefficients that are one or two orders of magnitude higher than the other copper-chloride complexes (Fig. 8a). Such high values of the molar absorptivity coefficients are not physically reasonable. Alternatively, assuming $b_{\gamma,[CuCl_2]^{0}_{aq}} = 0.40$ (or higher), $[CuCl_2]^{0}_{aq}$ is calculated to be a minor complex, also with unreasonably high absorptivity coefficients (Fig. 8c). Assuming an intermediate value of $b_{\gamma,[CuCl_2]^{0}_{aq}} = 0.10$, results in similar magnitude absorptivity coefficients for all copper-chloride complexes (Fig. 8b), suggesting that this value of the Setchénow coefficient is more consistent with our data. In any case, the values of the Setchénow coefficient was found to have a relatively small effect on the fitted log K values, that remain within the estimated uncertainties for a wide range of values on the coefficient ($0.05 < b_{\gamma,[CuCl_2]^{0}_{aq}} < 0.3$; Fig. 9).

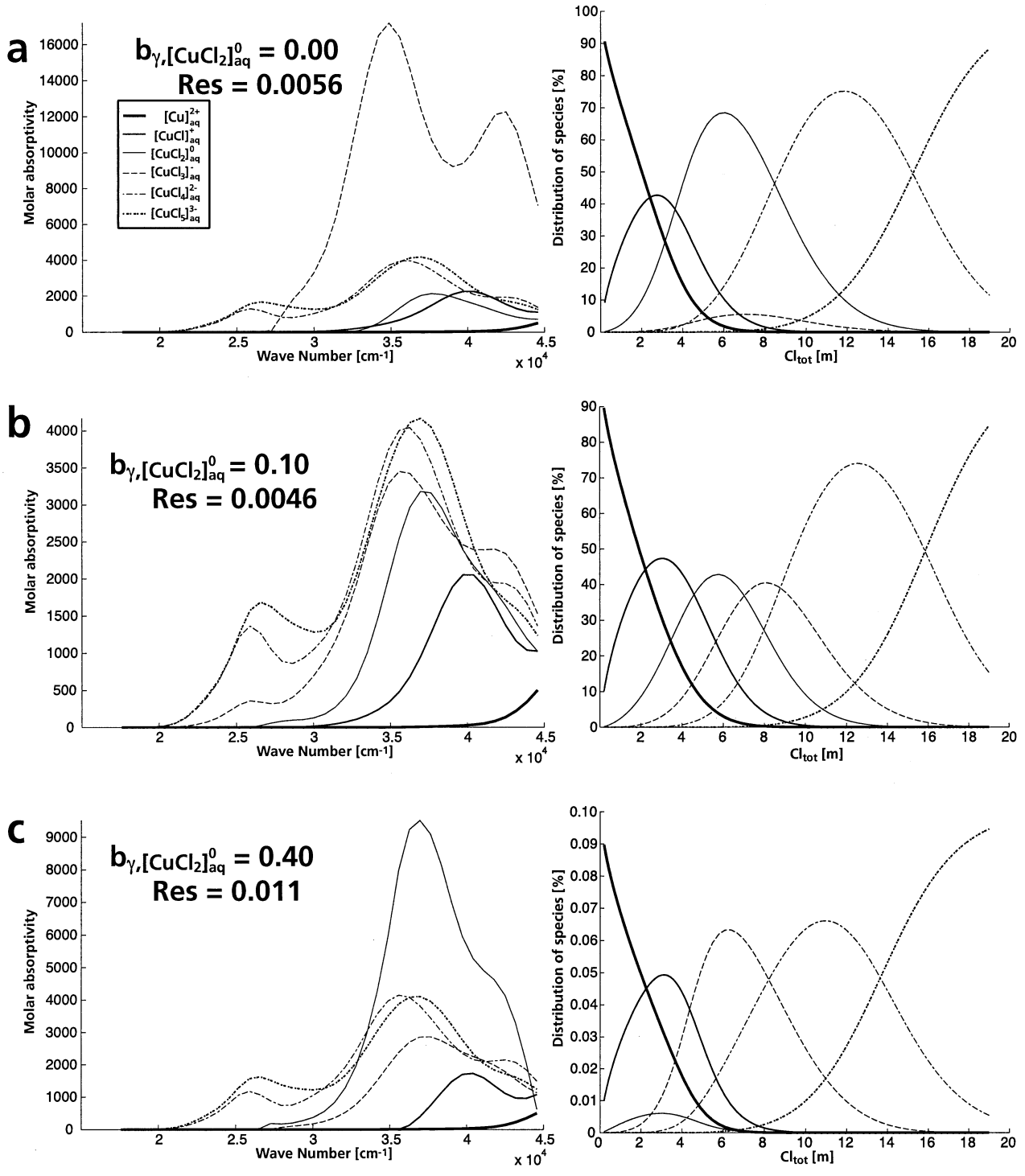

Fig. 8. Influence of the value of the Setchénow coefficient for $[CuCl_2]^0_{aq}$, $b_{\gamma[CuCl_2]^0_{aq}}$, on the fitted molar absorptivity coefficients and distributions of species (UV-Vis, 25°C).

Residual maps were calculated to examine the nature of the fits (i.e., single or multiple minima) and to estimate uncertainties in the fitted log K values. Residuals were calculated as a function of log K values and depicted as contours on log K versus log K sections (Fig. 10). In all cases there is only one minimum, although there is a large "flat-bottomed" valley around the minimum (example shown in Fig. 10). This is an inherent phenomenon in the analysis and interpretation of these types of experiments because the peaks for individual metal-halide complexes are usually broad and overlap, and there is a high level of co-linearity among aqueous species concentrations and among molar absorptivity coefficients for each spe-

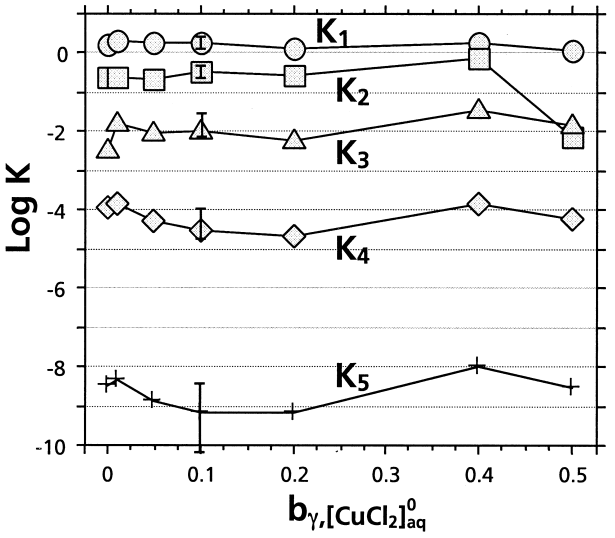

Fig. 9. Influence of the value of the Setchénow coefficient for $[CuCl_2]^0_{aq}$, $b_{\gamma[CuCl_2]^0_{aq}}$, on the fitted log K values (UV-Vis, 25°C).

cies. The residual contour corresponding to the 90% confidence level has been estimated using the equation and F-distribution factors given by Draper and Smith (1998; pp. 516 and 690). The confidence contour corresponding to 1.3 times the absolute minimum was used in all cases (range 1.25–1.35 depending on the number of absorbances taken into account, and the number of complexes). An example contour is depicted in Figure 10. The uncertainties listed in Table 4 correspond to the minimum and maximum values within the 90% confidence level.

4. DISCUSSION

In this section, the results obtained in this study are compared with those reported in previous studies, and the relative merits of our two alternative models (5- and 6-complex) are discussed. A large number of studies have been devoted to the speciation of Cu(II) in chloride-bearing aqueous brines at room temperature, using methods such as mineral solubility (e.g., Ramette, 1983), calorimetry (e.g., Arnek et al., 1982), and UV-Vis-NIR spectroscopy (e.g., Byrne et al., 1983; Bjerrum, 1987). However, most of these studies are restricted to one electrolyte and one ionic strength, and do not provide equilibrium constants for the Cu(II) complexes. We thus limit our comparison to the values derived from spectroscopic experiments by Bjerrum (1987), and the values presented by Sverjensky et al. (1997), which are based on the compilation of experimental data by Smith and Martell (1976). The only experimental studies on Cu(II)-chlorides complexes at temperatures higher than 35°C are qualitative spectroscopic studies (Kolonin and Aksenova, 1970; Sholz et al., 1972), and the recent EXAS experiments of Collings et al. (2000). In the absence of experimentally determined formation constants for the Cu(II)-chloro complexes, we compare our data with the theoretical estimates of Sverjensky et al. (1997). There are no data available to compare with for the possible $[CuCl_5]^{3-}$ complex in our 6-complex model, as previous studies only considered the 5-complex models.

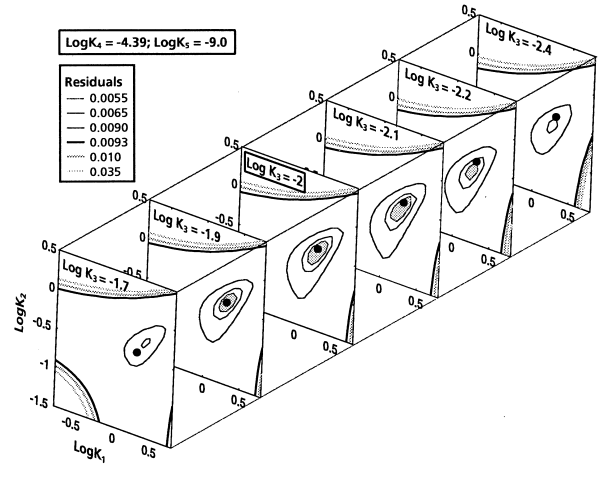

Fig. 10. Example of residual map at 25°C for the UV-Vis data set, 6-complex model. The maps represent a section through the 5-dimentional residual matrix, projected from the K_4 and K_5 values which lead the absolute minimum. The black dot represents the projection of the absolute minium in the mapped subspace. The greyed area indicates the 90% confidence level subspace.

At 25°C our results and those of Sverjensky et al. (1997) are in excellent agreement for most complexes and regardless of our 5- or 6-complex models (Table 4). Only the log K for $[CuCl_2]^0_{aq}$ (6-complex model) and $[CuCl_4]^{2-}_{aq}$ (5-complex model) are outside the 90% confidence level for our results. The results of Bjerrum (1987) for $[CuCl_3]^-_{aq}$ and $[CuCl_4]^{2-}_{aq}$ are outside of our estimated uncertainties; however, those results are presented as approximate. At 60°C the difference for $[CuCl]^+_{aq}$ is within 0.03 log units for both 5- and 6-complex models. For higher-order Cu-chloride complexes our 5-complex model agrees with Sverjensky et al. (1997) within approximately 0.5 log units. The results of our 6-complex model at 60°C show greater log K of formation for $[CuCl_2]^0_{aq}$ and higher order complexes, compared with those estimated from Sverjensky et al. (1997). At 90°C the comparison is similar, where agreement for $[CuCl]^+_{aq}$ is excellent and for higher order complexes the differences are up to 1 log unit (5-complex model). Again, our 6-complex model predicts higher log K of formation for all higher order complexes. In any case, both our 5- and 6-complex models predict the same trend with temperature for where the log K of formation increases with increasing temperature between 25°C and 90°C. The model of Sverjensky et al. (1997) for $[CuCl]^+_{aq}$, $[CuCl_2]^0_{aq}$ $[CuCl_3]^-_{aq}$ predicts lesser increases in log K of formation with increasing temperature, and for $[CuCl_4]^{2-}_{aq}$ their model predicts a decrease in log K of formation with increasing temperature.

Our two models lead to different predicted log K's of formation. Ideally, an independent method would allow us to distinguish between models. Recent EXAFS studies (D'Angelo et al., 1997; Collings et al., 2000) have attempted to quantify the number of chloride ligands around Cu(II) ions. In general, there is a poor agreement between the mean number of Cl-ligands in the first coordination sphere retrieved by fitting of EXAFS spectra and those predicted using thermodynamic properties from this and other studies (Fig. 11). This is probably a consequence of the complex chemistry of the Cu(II) ion. Interpreting the EXAFS spectra is complicated because the

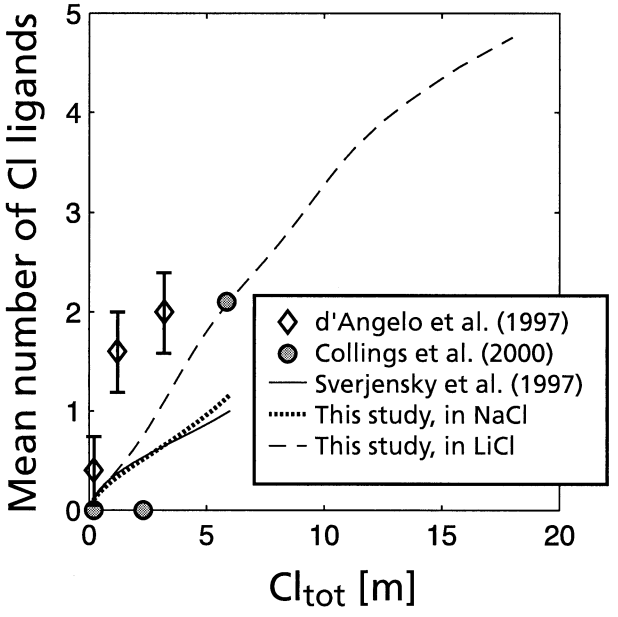

Fig. 11. Comparison of the mean number of Cl ligands in the first coordination shell of Cu(II) obtained by EXAFS (Collings et al., 2000; D'Angelo et al., 1997) with those calculated using thermodynamic data listed by Sverjensky et al. (1997) and those derived from this study. The calculations were performed for a NaCl solution using EQBRM, with Debye-Hückel parameters for NaCl dominated solutions from Helgeson et al. (1981), and a Cu(II) concentration of 0.1 m. The mean number of Cl ligands around Cu(II) in LiCl solutions retrieved in this study is plotted for reference.

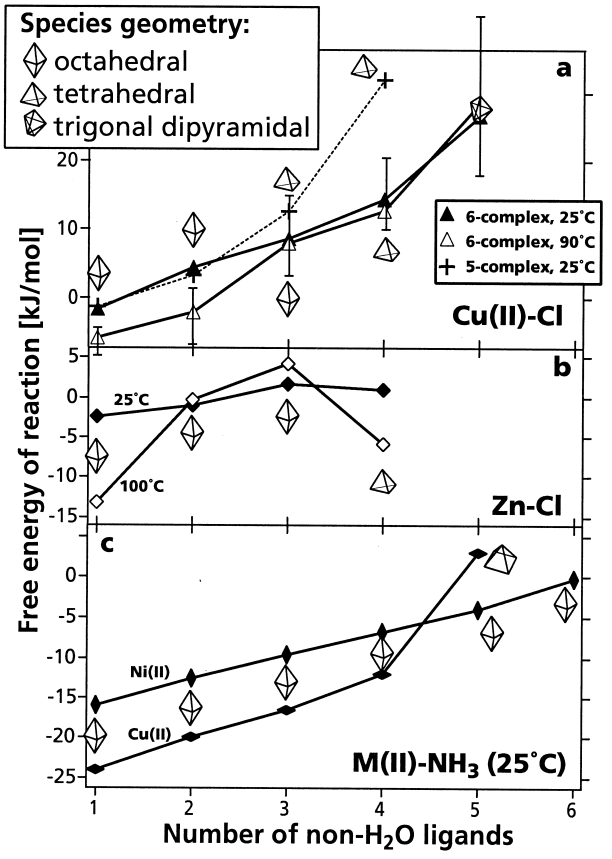

Fig. 12. Standard free energy of reaction for the successive addition of ligands to a complex (e.g., $ML_{x(aq)} + L_{(aq)} = ML_{x+1(aq)}$). (**a**) Cu(II)-Cl complexes, from this study. (**b**) Zn-Cl complexes, thermodynamic properties from Ruaya and Seward (1986); structural data quoted by Anderson et al. (1998). (**c**) Cu(II)-NH_3 and Ni(II)-NH_3 complexes (Gerloch and Constable, 1994).

contribution of the apical ligands to the EXAFS spectra is small, and thus extracting mean ligand numbers is a difficult task. Moreover, as is found in the solid state, the metal-ligand distances can vary for different coordination geometries (Fig. 6), and individual complexes cannot be isolated and analysed in these experiments.

Further insights may be possible by studying the energetics of the formation reactions of metal-ligand complexes. The standard Gibbs free energy of stepwise formation reactions, involving the replacement of a H_2O ligand in the first coordination sphere by a ligand L with no change in complex geometry, i.e.,

$$ML_x(OH_2)_{y(aq)} + L_{(aq)} = ML_{x+1}(OH_2)_{y-1(aq)} + H_2O_{(1)} \quad (21)$$

usually increases as the number of ligands increases (e.g., Ni(II)-NH_3 ligands; Figure 12c). This results from the decrease in the number of H_2O groups that can be replaced by a ligand as the number of bound ligands increases (entropy contribution). A deviation from this trend usually points to a change in the structure and bonding at the metal centre (e.g., Shriver et al., 1996), such as the octahedral to tetrahedral transition that occurs for most halide complexes of divalent transition metals such as Co(II), Fe(II), Ni(II) and Zn(II) (e.g., Susak and Crerar, 1984). This change in stereochemistry is mainly driven by the ligand-ligand repulsion between the halide ligands and by a favourable entropy change, resulting from the release of three coordinated water ligands into solution, and not one as in the process of simply replacing one H_2O (Eqn. 21):

$$ML_3(OH_2)_{3(aq)} + L_{(aq)} = ML_{4(aq)} + 3H_2O_{(1)} \quad (22)$$

For transition-metal-halide complexes that do not exhibit the Jahn-Teller effect, the stepwise formation constants for the sequential coordination of halide ligands to the metal centre decrease (i.e., $K_1 > K_2 > K_3$) with the addition of the first three ligands and then rise abruptly when the fourth halide is added (e.g., Zn-Cl system; Fig. 12b). In keeping with this, many tetrahedral complexes of the form $[MX_4]^{2-}$ have been isolated, indicating that they can be generated in sufficient concentration in solution to be crystallised. On the other hand, examples of complexes of the type $[MCl_3(OH_2)_3]^-$ are quite rare.

The free energies of reaction calculated for the 5-complex model do not show the same trend as for other transition metal complexes, where there is no abrupt change between octahedral and tetrahedral complexes. In addition, there is an increase in the free energy of reaction, in contrast to that observed in other transition metal complexes. For the 6-complex model, the predicted free energies of reaction display a consistent trend from $[CuCl]^{aq}_{+}$ to $[CuCl_4]^{aq}_{2-}$ (Fig. 12a), although the spectral characteristics clearly indicate a change in the geometry of the

complex between $[CuCl_3(OH_2)_3]^-$ and $[CuCl_4]^{2-}$. The free energy of the next stepwise formation reaction ($[CuCl_5]^{3-}$) appears to increase more than the free energies of lower-order complexes. This suggests another change in the geometry of the complex, as also supported by the spectral characteristic of the species. This behaviour probably results from the Jahn-Teller effect, and is in keeping with observations in the well-studied Cu(II)-NH_3-H_2O system (e.g., Hathaway and Tomlinson, 1970). More NH_3 molecules enter the coordination sphere of Cu(II) as the concentration of NH_3 increases. The geometry of $[Cu(NH_3)_x(OH_2)_{6-x}]^{2+}$ complexes is distorted octahedral for x between 0 and 4, but changes for the next member in the series. EXAFS and electronic spectroscopy studies have shown that $[Cu(NH_3)_5]^{2+}$ does not have a H_2O group in the first coordination shell, and probably adopts a square pyramidal geometry (Sano et al., 1984; Valli et al., 1996). The free energy for the addition of the 5th NH_3 is higher than expected from the trend shown by the previous replacement reactions (Fig. 12c), similar to what we observed for the formation of $[CuCl_5]^{3-}$.

Although we still cannot choose unequivocally between the 5- and 6-complex models, the indirect evidence suggests that the 6-complex model is more likely. The evidence includes the very close match between the solid-state spectra of $[CuCl_4]^{2-}$ and that of $[CuCl_4]^{2-}_{aq}$ in the 6-complex model, and the fact that crystals containing the $[CuCl_4]^{2-}$ and $[CuCl_5]^{3-}$ complexes can be easily precipitated from aqueous electrolyte solutions, suggesting that these complexes exist in significant amounts in the aqueous phase.

5. APPLICATION

The properties derived in this study can be used to understand the speciation, transport and deposition of copper in geological and other environments. There are many possible copper complexes (e.g., chloride, sulphide, sulphate, amine) in natural and contaminated waters and brines. Copper(II) chloride complexes are likely to be important in oxidised waters and brines with high chloride concentrations, such as in evaporitic playa lakes and seas, evaporite-bearing sedimentary basins (e.g., red bed copper mineralisation; Sverjensky, 1987), hypersaline soils, mine drainage waters (e.g., Atacama desert) and supergene and other weathering environments. Recent advances in ore processing and mining technologies have resulted in a renewed interest for oxidised copper deposits. The supergene enrichment of copper in at least some of these deposits was the result of circulation of oxidised chloride brines (e.g., Quast, 2000). In large massive sulphide deposits, the supergene alteration can occur at temperatures as high as ~60°C, due to the heat generated by sulfide oxidation during weathering (Melchiorre et al., 1999).

As an example application of our results we show activity-activity diagrams that depict copper speciation and copper mineral solubility as a function of redox (log $f_{H2(g)}$) and chloride activity at temperatures of 25°C and 90°C (Fig. 13). The thermodynamic properties for Cu(II)-chloride complexes are from this study (6-complex model), those for Cu(I)-chlorides are from Xiao et al. (1998), and those for other aqueous species and minerals are from Johnson et al. (1992). There are three important aspects to note. First, the predominance areas for Cu(II)-chloride complexes shift to lower chloride activity with increasing temperature (Fig. 13). This means that the solubility of copper minerals will be more sensitive to changes in chloride activities and concentrations (i.e., salinity) at higher temperature, especially in oxidised and highly saline brines with high chloride activities where $[CuCl_3]^-_{aq}$ and/or $[CuCl_4]^{2-}_{aq}$ predominate. Second, the predominance areas of Cu(I)-chloride complexes expand at the expense of Cu(II)-chloride complexes as temperature increases to 90°C from 25°C (Fig. 13). This shows that Cu(I)-chloride complexes become increasingly important, relative to Cu(II)-chloride complexes, as temperature increases to at least approximately 100°C, although Cu(II)-chloride complexes will predominate over Cu(I)-chloride complexes in near-surface oxidised chloride brines. Third, the solubilities of native copper, cuprite and atacamite increase with increasing temperature (prograde solubility) as reflected in their smaller stability fields at 90°C; however, tenorite is predicted to have retrograde solubility (predicted stability field at 90°C but not at 25°C for the chosen conditions of the diagrams). For more complicated applications (e.g., environments with sulphur, amine and other ligands, as well as other metals), the properties derived in this study can be used to predict the relative importance of chloride and other types of copper complexes.

6. CONCLUSIONS

The UV-Vis-NIR absorbance spectra of Cu(II)-chloride complexes were measured at 25°C, 60°C, and 90°C in acidic solutions containing between 0 to 18 m LiCl. Thermodynamic properties (log K) of the reactions between Cu(II)-chloride complexes were fitted to the spectra, with residuals at the level of the analytical error, using two different models that assume the presence of 5 or 6 Cu(II)-chloro-aqua complexes. A 6-complex model, containing distorted octahedral $[Cu(OH_2)_6]^{2+}$, $[CuCl(OH_2)_5]^+$, $[CuCl_2(OH_2)_3]^0$, and (probably also distorted octahedral) $[CuCl_3(OH_2)_2]^-$, distorted tetrahedral $[CuCl_4]^{2-}$, and dipyramidal trigonal $[CuCl_5]^{3-}$, is favoured because of indirect evidence for the stability of the latter two complexes. In general (e.g., independently of the speciation model chosen), the formation constants of the Cu(II)-chloride complexes are higher than previous estimates (e.g., Sverjensky et al., 1997), indicating that the Cu(II)-chloride complexes are more stable than previous studies suggest.

This study shows that the quantitative interpretation of UV-Vis-NIR data depends upon the choice of the chemical speciation model (i.e., nature of the complexes present in aqueous solution, and a model for activity coefficients). In this context, it is important to evaluate the data carefully before setting up the speciation model (what information does the dataset really contain?), and to use available constraints from other sources. A combination of numerical techniques is also important in interpreting the spectral data. PCA is a standard method in spectroscopy, but new methods of "model-free" analysis were found to be extremely useful in this study. The concentration profiles and molar absorptivity spectra yielded by "model-free" analysis are independent of any speciation model, and the results can be used to set up reasonable initial guesses for the quantitative analysis with a speciation model. The final choice of the speciation model, however, must integrate this information with results from other methods, as well as with constraints from coordination chemistry.

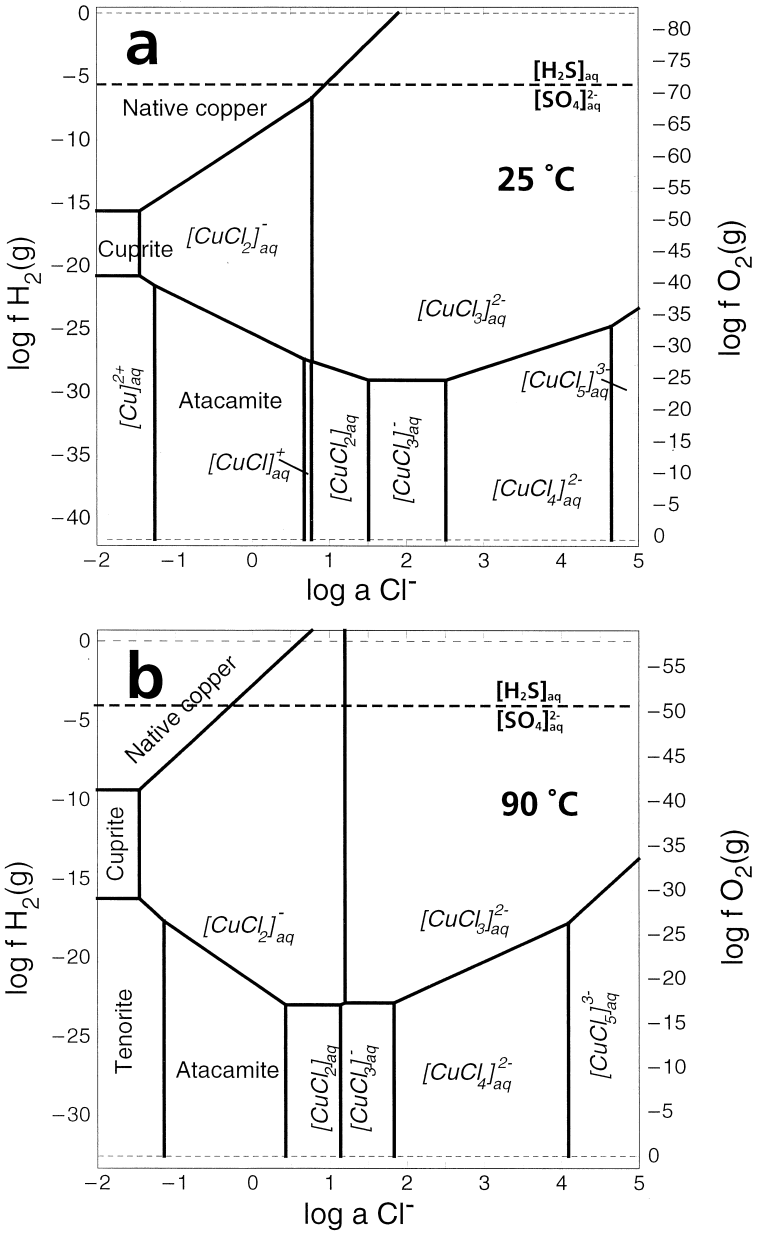

Fig. 13. Activity-Activity diagrams for Cu speciation in chloride brine drawn at pH = 5 and for activities of copper species of 0.005. Data for Cu(II) chlorides from this study (6-complex model), for Cu(I) chlorides from Xiao et al. (1998), and for other aqueous species and minerals from Johnson et al. (1992). The redox state is indicated both in terms of the fugacity of $H_{2(g)}$ (on the left side) and $O_{2(g)}$ (on the right side). The sulfate/bisulfide predominance fields (thick dashed line) and the water stability boundaries (thin dashed lines) are indicated for reference.

UV-Vis-NIR spectrophotometry has several advantages over solubility experiments, although ideally a combination of experimental techniques should be used to confirm and/or extend results from independent techniques. UV-Vis-NIR spectroscopy provides an insight into the stoichiometry and geometry of the complexes present in solution, and allows wider range of solution compositions to be investigated. For example, in this study, we have applied UV-Vis-NIR spectrophotometry to studying solutions with quite low Cu(II) concentrations ($\sim 5 \times 10^{-4}$ molal). This means that UV-Vis-NIR spectroscopy can be used to gain insight into the speciation of trace metals in highly concentrated brines (>2 m). The distribution of the Cu-complexes in such brines can be retrieved using "model-free" analysis, without the need for a thermodynamic model. In simple systems (one trace element in a 1–1 electrolyte), it is possible to obtain values of the thermodynamic stability constants of the complexes that are compatible with existing modelling software based on Helgeson's formalism (Helgeson and Kirkham, 1974a; 1974b; Helgeson et al., 1981) at moderate salt concentration, but which can be extended to high concentrations.

Cu(II) chloro-complexes, in particular distorted octahedral

$[CuCl_2(OH_2)_4]^0$ and distorted tetrahedral $[CuCl_4]^{2-}$, will control copper transport and deposition in nature in oxidising, near-surface environments where chloride-activities are high, such as evaporite-bearing sedimentary basins or hypersaline soils. The geometry of the complexes in the aqueous solution strongly influences the mechanisms and kinetics of coprecipitation and sorption of metals. Thus, the behaviour of Cu(II) in chloride brines is probably affected by the octahedral-tetrahedral transition.

Acknowledgments—Thanks are due to Oleg Suleimenov (ETH Zürich) for introducing me (JB) to the MatLab programming environment, and to Anna de Juan (University of Barcelona) for helping with the "model-free" analysis. The manuscript benefited from the reviews of three anonymous reviewers, and from helpful comments from the GCA editors, Eric Oelkers and Frank Podosek. This work has been supported by an Australian Research Council Large Grant (DMcP), and by fellowships from the Monash University Research Fund and from the Swiss National Science Foundation.

Associate editor: E. H. Oelkers

REFERENCES

Allen G. C. and Hush N. S. (1967) Reflectance spectrum and electronic states of $CuCl_5^{3-}$ ion in a number of crystal lattices. *Inorg. Chem.* **6,** 4–8.

Alpert N. L. (1973) IR: Theory and practice of infrared spectroscopy. Plenum/Rosetta.

Anderson A. J., Mayanovic R. A., and Bajt S. (1998) A microbeam XAFS study of aqueous chlorozinc complexing to 430°C in fluid inclusions from the Knaumühle granitic pegmatite, Saxonian granulite facies, Germany. *Can. Mineral.* **36,** 511–524.

Anderson G. M., Castet S., Schott J., and Mesmer R. E. (1991) The density model for estimation of thermodynamic parameters of reactions at high temperatures and pressures. *Geochim. Cosmochim. Acta.* **55,** 1769–1779.

Anderson G. M. and Crerar D. A. (1993) Thermodynamics in Geochemistry. Oxford University Press.

Antolini L., Marcotrigiano G., Menbue L., and Pellacani G. C. (1980) Spectroscopic and structural investigation on the pentachloro- and (mixed-pentahalo) cuprates(II) of the *N*-(2-ammoniumethyl) piperazinium cation. The first case of monomeric pentahalocuprate(II) having square-pyramidal structure. Crystal and molecular structure of the *N*-(2-ammoniumethyl) piperazinium pentachlorocuprate(II) dihydrate. *J. Am. Chem. Soc.* **102,** 1303–1308.

Arnek R., Puigdomenech I., and Valiente M. (1982) A calorimetric study of Copper(II) chloride complexes in aqueous solution. *Acta Chemica Scandinavia* **A36,** 15–19.

Bebie J., Seward T. M., and Hovey J. K. (1998) Spectrophotometric determination of the stability of thallium(I) chloride complexes in aqueous solutions up to 200°C. *Geochim. Cosmochim. Acta.* **62,** 1643–1651.

Bentouhami E., Khan M. A., Meullemeestre J., and Vierling F. (1992) Stability and electronic spectra of copper(II) halides in butan-1-ol and the effects of R-OH type solvents on these properties. *Polyhedron.* **17,** 2179–2182.

Bjerrum J. (1987) Determination of small stability constants. A spectroscopic study of copper(II) chloride complexes in hydrochloric acid. *Acta Chemica Scandinavica* **A41,** 328–334.

Bogatykh S. A. and Evnovitch I. D. (1965) Investigation of densities of aqueous LiBr, LiCl, and $CaCl_2$ solutions in relation to conditions of gas drying. *Zh. Prikl. Khim.* **38,** 945.

Burns P. C. and Hawthorne F. C. (1993) Tolbachite, $CuCl_2$, the first example of Cu^{2+} octahedrally coordinated by Cl^-. *Am. Mineral.* **78,** 187–189.

Byrne R. H., Van der Weijden C., Kester D. R., and Zuehlke R. W. (1983) Evaluation of the $CuCl^+$ stability constant and molar absorptivity in aqueous media. *J. Sol. Chem.* **12,** 581–595.

Collings M., Sherman D. M., and Ragnarsdottir K. V. (2000) Complexation of Cu^{2+} in oxidised NaCl brines from 25°C to 175°C: Results from in situ EXAFS spectroscopy. *Chem. Geol.* **167,** 65–73.

Crerar D. A., Wood S., Brantley S., and Bocarsly A. (1985) Chemical controls on solubility of ore-forming minerals in hydrothermal systems. *Can. Mineral.* **23,** 333–352.

D'Angelo P., Bottari E., Festa M. R., Nolting H.-F., and Pavel N. V. (1997) Structural investigation of copper(II) chloride solutions using x-ray absorption spectroscopy. *J. Chem. Phys.* **107,** 2807–2812.

De Juan A. and Tauler R. (1999) Multiple Curve Resolution Home Page (http://www.ub.es/gesq/mcr/mcr.htm).

De Juan A., Vander Heyden Y., Tauler R., and Massart D. L. (1997) Assessment of new constraints applied to the alternating least squares method. *Anal. Chim. Acta.* **346,** 307–318.

Desjardins S. R., Penfield K. W., Cohen S. L., Musselman R. L., and Solomon E. I. (1983) Detailed absorption, reflectance, and UV photoelectron spectroscopic and theoretical studies of the charge-transfer transitions of $CuCl_4^{2-}$:Correlation of the square-planar and the tetrahedral limits. *J. Am. Chem. Soc.* **105,** 4590–4603.

Djabi F., Meullemeestre J., Vierling F., Bouet G., and Ahmed Khan M. (1994) Chlorocomples du cuivre(II) dans le propan-1-ol et le butan-2-ol. Effet de la position du groupement OH. *Bull. Soc. Chim. Fran.* **131,** 53–57.

Draper N. R. and Smith H. (1998) Applied regression analysis. John Wiley & Sons.

Driesner T., Seward T. M., and Tironi I. G. (1998) Molecular dynamics simulation study of ionic hydration and ion association in dilute and 1 molal aqueous sodium chloride solutions from ambient to supercritical conditions. *Geochim. Cosmochim. Acta.* **62,** 3095–3107.

Finney J. J., Graeber E. J., Rosenzweig A., and Hamilton R. D. (1977) The structure of chloroxiphite, $Pb_3CuO_2(OH)_2Cl_2$. *Min. Mag.* **41,** 357–361.

Furlani C. and Morpurgo G. (1963) Properties and electronic structure of tetrahalogenocuprate (II)-complexes. *Theoret. Chim. Acta.* **1,** 102–115.

Gampp H., Maeder M., Meyer C. J., and Zuberbühler A. D. (1985) Calculation of equilibrium constants from multiwavelength spectroscopic data—III. *Talanta.* **32,** 1133–1139.

Gates J. A. and Wood R. H. (1985) Densities of aqueous solutions of NaCl, $MgCl_2$, KCl, NaBr, LiCl, and $CaCl_2$ from 0.05 to 5.0 mol kg^{-1} and 0.1013 to 40 MPa at 298.15 K. *J. Chem. Eng. Data* **30,** 44.

Gerloch M. and Constable E. C. (1994) Transition Metal Chemistry. VCH Verlagsgesellschaft, Weinheim, Germany.

Gu Y., Gammons C. H., and Bloom M. S. (1994) A one-term extrapolation method for estimating equilibrium constants of aqueous reactions at elevated temperatures. *Geochim. Cosmochim. Acta.* **58,** 3545–3560.

Harker D. (1936) The crystal structure of cupric chloride dihydrate $CuCl_2(H_2O)_2$. *Zeit. Kristallograph., Kristallgeo., Kristallphys., Kristallchem.* **93,** 136–145.

Harvie C. E., Moller N., and Weare J. H. (1984) The prediction of mineral solubilities in natural waters: The Na-K-Mg-Ca-H-Cl-SO_4-OH-HCO_3-CO_3-CO_3-CO_2-H_2O system to high ionic strengths at 25°C. *Geochim. Cosmochim. Acta.* **48,** 723–751.

Hatfield W. E., Bedon H. D., and Horner S. M. (1965) Molecular orbital theory for the pentachlorocuprate(II) ion. *Inorg. Chem.* **4,** 1181–1184.

Hathaway B. J. and Tomlinson A. A. G. (1970) Copper(II) ammonia complexes. *Coord. Chem. Rev.* **5,** 1–43.

Heinrich C. A. and Seward T. M. (1990) A spectrophotometric study of aqueous iron (II) chloride complexing from 25 to 200°C. *Geochim. Cosmochim. Acta.* **54,** 2207–2221.

Helgeson H. and Kirkham D. H. (1974a) Theoretical prediction of the thermodynamic behavior of aqueous electrolytes at high pressures and temperatures: I. Summary of the thermodynamic/electrostatic properties of the solvent. *Am. J. Sci.* **274,** 1089–1.

Helgeson H. and Kirkham D. H. (1974b) Theoretical prediction of the thermodynamic behavior of aqueous electrolytes at high pressures and temperatures: II. Debye-Hückel parameters for activity coefficients and relative partial molal properties. *Am. J. Sci.* **274,** 1199–1261.

Helgeson H., Kirkham D. H., and Flowers G. C. (1981) Theoretical prediction of the thermodynamic behavior of aqueous electrolytes at high pressures and temperatures: IV. Calculation of activity coeffi-

cients, osmotic coefficients, and apparent molal and standard and relative partial molal properties to 600°C and 5 kb. *Am. J. Sci.* **281,** 1249–1516.

Helz G. R., Charnock J. M., Vaughan D. J., and Garner C. D. (1993) Multinuclearity of aqueous copper and zinc bisulfide complexes: An EXAFS investigation. *Geochim. Cosmochim. Acta.* **57,** 15–25.

Holmes H. F. and Mesmer R. E. (1983) Thermodynamic properties of aqueous solutions of the alkali metal chlorides to 250°C. *J. Phys. Chem.* **87,** 1242–1255.

Isono T. (1984) Density, viscosity, and electrolytic conductivity of concentrated aqueous electrolyte solutions at several temperatures. Alkaline-earth chlorides, $LaCl_3$, Na_2SO_4, $NaNO_3$, NaBr, KNO_3, KBr, and $Cd(NO_3)_2$. *J. Chem. Eng. Data* **29,** 45.

Johnson J. W., Oelkers E. H., and Helgeson H. C. (1992) SUPCRT92: A software package for calculating the standard molal thermodynamic properties of minerals, gazes, aqueous species and reactions from 1 to 5000 bars and 0° to 1000° C. *Comput. Geosci.* **18,** 899–920.

Jones G. and Bradshaw B. C. (1932) The transference number of lithium chloride as a function of the concentration. *J. Am. Chem. Soc.* **54,** 138.

Kielland J. (1937) Individual activity coefficients of ions in aqueous solutions. *J. Am. Chem. Soc.* **59,** 1675–1678.

Kolonin G. R. and Aksenova T. P. (1970) Investigation of complexing of some heavy metals in NaCl solutions at 20–90°C. *Geochem. Int.* **11,** 973–978.

Legget D. J. (1977) Numerical interpretation of multi-component spectra. *Anal. Chem.* **49,** 276–281.

Legget D. J. and McBryde W. A. E. (1975) General computer program for the computation of stability constants from absorbance data. *Anal. Chem.* **47,** 1065–1070.

Lengyel S., Tamás J., Giber J., and Holderith J. (1964) Study of viscosity of aqueous alkali halide solutions. *Acta Chim. Acad. Sci. Hung.* **40,** 125.

Malinowski E. R. (1977) Determination of the number of factors and the experimental error in a data matrix. *Anal. Chem.* **49,** 612–616.

Malinowski E. R. and Howery D. G. (1980) Factor analysis in chemistry. John Wiley & Sons.

McGinnety J. A. (1972) Cesium tetrachlorocuprate. Structure, crystal forces, and charge distribution. *J. Am. Chem. Soc.* **94,** 8406–8413.

Melchiorre E. B., Criss R. E., and Rose T. P. (1999) Oxygen and carbon isotope study of natural and synthetic malachite. *Econ. Geol.* **94,** 245–259.

Millero F. J. and Hawke D. J. (1992) Ionic interactions of divalent metals in natural waters. *Mar. Chem.* **40,** 19–48.

Millero F. J., Ward G. K., and Chetirkin P. V. (1977) Relative sound velocities of sea salts at 25°C. *J. Acoust. Soc. Am.* **61,** 1492.

Millero F. J., Yao W. S., and Aicher J. (1995) The speciation of Fe(II) and Fe(III) in natural waters. *Mar. Chem.* **50,** 21–39.

Nelder J. A. and Mead R. (1965) A simplex method for function minimisation. *The Comp. J.* **7,** 308–313.

Neumaier A. (1998) MINQ - General definite and bound constrained indefinite quadratic programming. WWW document, http://solon.cma.univie.ac.at/~neum/software/minq/.

Oelkers E. H. and Helgeson H. C. (1993) Multiple ion association in supercritical aqueous solutions of single electrolytes. *Sci.* **261,** 888–891.

Ostroff A. G., Snowden B. S., and Woessner D. E. (1969) Viscosities of protonated and deuterated water solutions of alkali metal chlorides. *J. Phys. Chem.* **73,** 2784.

Out D. and Los J. M. (1980) Viscosity of aqueous solutions of univalent electrolytes from 5 to 95°C. *J. Sol. Chem.* **9,** 19–35.

Pitzer K. S. (1973) Thermodynamics of electrolytes. I. Theoretical basis and general equations. *J. Phys. Chem.* **77,** 268–277.

Pokrovskii V. A. and Helgeson H. C. (1997) Calculation of the standard partial molal thermodynamic properties of KCl^0 and activity coefficients of aqueous KCl at temperatures and pressures to 1000°C and 5 kbar. *Geochim. Cosmochim. Acta.* **61,** 2175–2183.

Quast K. B. (2000). Leaching of atacamite ($Cu_2(OH)_3Cl$) using dilute sulphuric acid. *Min. Eng.* **13,** 1647–1652.

Ramette R. W. (1983) Copper(II) chloride complex equilibrium constants. *Inorg. Chem.* **22,** 3323–3326.

Raymond K. N., Meek D. W., and Ibers J. A. (1968) The structure of hexaamminechromium(III) pentachlorocuprate(II), $(Cr(NH_3)_6)(CuCl_5)$. *Inorg. Chem.* **7,** 1111–1117.

Roedder E. (1976) Fluid-inclusion evidence on the genesis of ores in sedimentary and volcanic rocks. In *Handbook of strata-bound and stratiform ore deposits* (ed. K. H. Wolf), pp. 67–110. Elsevier.

Ruaya J. R. and Seward T. M. (1986) The stability of chlorozinc(II) complexes in hydrothermal solutions up to 350°C. *Geochim. Cosmochim. Acta.* **50,** 651–661.

Sano M., Maruo T., Masuda Y., and Yamatera H. (1984) Structural study of copper(II) sulfate solution in highly concentrated aqueous ammonia by X-ray absorption spectra. *Inorg. Chem.* **23,** 4466–4469.

Saurina J., Hernández-Cassou S., and Tauler R. (1995) Multivariate curve resolution applied to continuous-flow spectrophotometric titrations. Reaction between amino acids and 1,2-naphthoquinone-4-sulfonic acid. *Anal. Chem.* **67,** 3722–2726.

Setchénow M. (1889) Über die Konstitution der Salzlösungen auf Grund ihres Verhaltens zu Kohlensaure. *Zeit. Physikal. Chem.* **4,** 117–126.

Sholz H., Ludeman H. D., and Franck E. U. (1972) Spectra of Cu(II)-complexes in aqueous solutions at high temperatures and pressures. *Bunsen Gesell. Physikal. Chem. Ber.* **76,** 406–409.

Shriver D. F., Atkins P. W., and Langford C. H. (1996) Inorganic Chemistry Oxford University Press.

Smith D. W. (1976) Chlorocuprates(II). *Coord. Chem. Rev.* **21,** 93–158.

Suhrmann R. and Wiedersich I. (1953) The effect of foreign ions on the conductivity of hydrogen ion in aqueous solutions. *Z. Annorg. Allg. Chem.* **272,** 167.

Susak N. and Crerar D. A. (1984) Spectra and coordination changes of transition metals in hydrothermal solutions: Implications for ore genesis. *Geochim. Cosmochim. Acta.* **49,** 555–564.

Sverjensky D. A. (1987) The role of migrating oil field brines in the formation of sediment-hosted Cu-rich deposits. *Econ. Geol.* **82,** 1130–1141.

Sverjensky D. A., Shock E. L., and Helgeson H. C. (1997) Prediction of the thermodynamic properties of aqueous metal complexes to 1000°C and 5 kb. *Geochim. Cosmochim. Acta.* **61,** 1359–1412.

Tauler R. and Casassas E. (1989) Application of principal component analysis to the study of multiple equilibria systems. Study of Copper(II)/Salicylate/Mono-, Di- and Triethanolamine systems. *Anal. Chim. Acta.* **223,** 257–268.

Tauler R. and Casassas E. (1992) Application of factor analysis to speciation in multi-equilibria systems. *Analusis.* **20,** 255–268.

Thompson R. A. and Helz G. R. (1994) Copper speciation in sulfidic solutions at low sulfur activity—further evidence for cluster complexes? *Geochim. Cosmochim. Acta.* **58,** 2971–2983.

Ulrich T., Günther D., and Heinrich C. A. (1999) Gold concentrations of magmatic brines and the metal budget of porphyry copper deposits. *Nature.* **399,** 676–679.

Valli M., Matsuo S., Wakita H., Yamaguchi T., and Nomura M. (1996) Solvation of copper(II) ions in liquid ammonia. *Inorg. Chem.* **35(19),** 5642–5645.

Xiao Z., Gammons C., and Williams-Jones A. (1998) Experimental study of copper(I) chloride complexing in hydrothermal solutions at 40 to 300°C and saturated water vapor pressure. *Geochim. Cosmochim. Acta.* **62,** 2949–2964.